

ACCRETION DISKS AROUND T TAURI STARS¹

CLAUDE BERTOUT² AND GIBOR BASRI³
 Astronomy Department, University of California at Berkeley

AND

JEROME BOUVIER
 Institut d'Astrophysique de Paris

Received 1987 August 17; accepted 1987 December 17

ABSTRACT

We examine in some theoretical and observational detail the proposition that many T Tauri stars are still actively accreting material from a surrounding disk of material formed at the same time as the star in the gravitational collapse of a rotating molecular core. We find that a simple disk model can explain the general features of the spectral shape of the continuum from the ultraviolet to the infrared, and that the observations are both unified and explained if classical T Tauri stars are chromospherically active pre-main-sequence stars with accretion disks. The theory employed is an extension of the pioneering work of Lynden-Bell and Pringle; this can be reduced to a description of the disk and accompanying boundary layer (where the disk meets the star) with very few free parameters. Contemporaneous optical and ultraviolet observations, along with extensive photometric monitoring in the optical and infrared, are used to test these models and show that there is evidence for accretion in the range 5×10^{-8} – $5 \times 10^{-7} M_{\odot} \text{ yr}^{-1}$ from stars exhibiting strong ultraviolet excesses. The models which explain the UV excess are also quite successful with the infrared spectrum shortward of $10 \mu\text{m}$ and with the total system luminosities observed. We use stars with comparatively little evidence of disks to establish the extent to which the chromosphere contributes to the ultraviolet excess. We characterize the important properties of the disks and suggest further work which can test this paradigm. Some of the remaining problems in fully understanding T Tauri spectra are discussed.

Subject headings: stars: pre-main-sequence — stars: accretion — spectrophotometry

I. INTRODUCTION

Our solar system's morphology suggests that the primitive solar nebula once had a disklike structure; hence it has long been suspected that stellar formation proceeds anisotropically. Unfortunately, we are not yet in a position to quantitatively understand the formation of either the primitive solar nebula or the Sun. While the formation of a solar-type protostar from the diffuse cloud stage to the stellar stage has been computed with complex hydrodynamic evolution codes in the case of zero angular momentum (cf. Winkler and Newman 1980*a, b*), the additional degree of complexity introduced by relaxing the assumption of spherical symmetry renders it impossible to follow numerically all but the earliest, isothermal phases of gravitational collapse. Various axisymmetric and asymmetric hydrodynamic computations of the gravitational collapse of diffuse clouds, using initial values of specific angular momentum compatible with galactic differential rotation ($J/M \approx 10^{24} \text{ cm}^2 \text{ s}^{-1}$) usually result in a ring that is unstable to fragmentation (see the review by Bodenheimer 1983).

There is, however, growing observational evidence that low-mass stars are not formed directly from the gravitational collapse of a diffuse cloud, but rather from the contraction of cores with typical densities $\sim 10^4 \text{ cm}^{-3}$ and radii $\sim 0.1 \text{ pc}$ observed in many giant molecular clouds (Myers and Benson

1983). Terebey, Shu, and Cassen (1984) used a semianalytical computational method to follow the evolution of an initially slowly rotating configuration with properties comparable to those of cloud cores (with angular velocity $\approx 10^{-14} \text{ s}^{-1}$ and $J/M \approx 10^{21} \text{ cm}^2 \text{ s}^{-1}$). They found that a large fraction of the core mass forms a central star, while matter with higher specific angular momentum accumulates onto a disk. In a different approach, Tscharnuter (1985) used a full hydrodynamic code in which he included turbulent friction in a parametrized way to study the collapse of a $3 M_{\odot}$ slowly rotating core, which ended in the formation of a disk surrounding a $0.5 M_{\odot}$ star. Recently, Boss (1987) computed the evolution of an isothermal rotating cloud for a variety of initial conditions and found that accretion always proceeds faster along the rotation axis, resulting in the formation of a central protostar surrounded by a disk perpendicular to a narrow, depleted region surrounding the rotation axis. This suggests that channeling of the stellar wind in bipolar regions is a natural consequence of the protostellar collapse. He mentions, however, that this result is at least partially due to the particular boundary condition of fixed volume used in the computation, which will of course apply best to the case where the star is formed by the collapse of an individual, well-defined globule. Indeed his results contrast with the case computed by Terebey, Shu, and Cassen (1984), who assume continuous accretion of matter located in the molecular cloud surrounding the protostar.

Because of the various simplifying assumptions required in the computations mentioned above, the exact nature of the optically thick disk surrounding the developing protostar is still largely unknown. Present results seem however consistent with the idea that the disk should be Keplerian in the phase

¹ Research reported herein is based in part on data collected at the European Southern Observatory, La Silla, Chile, and in part on data from the Lick Observatory run by the University of California.

² Also Laboratoire d'Astrophysique Théorique du Collège de France and Institut d'Astrophysique de Paris.

³ Guest Observer, *International Ultraviolet Observatory* (NASA).

preceding planet formation, as assumed in many models of solar nebulae (cf. Lin and Papaloizou 1985; Morfill, Tscharnuter, and Völk 1985).

Molecular observations of large-scale, flattened structures have been reported around a number of massive pre-main-sequence objects (e.g., Bieging 1984), but limited resolution is still an obstacle to the discovery of smaller structures. A solar-system sized disk of say 100 AU diameter located in the Taurus cloud has an angular diameter of $0''.6$, while the resolution limit of current millimetric interferometers is about $6''$ at 110 GHz. The smallest structure detected so far is the *Keplerian* disk with diameter about 4000 AU and mass about $0.1 M_{\odot}$ around the T Tauri star HL Tauri (Sargent and Beckwith 1987).

We must therefore rely on indirect evidence for inferring the presence of smaller disks around other low-mass young stellar objects. One such indirect clue is the presence of blue-displaced forbidden lines in the spectra of numerous T Tauri stars. Forbidden lines are formed in low-density, ionized regions, and therefore probe the outer parts of the stellar wind far away from the star. As first noticed by Appenzeller, Jankovics, and Oestreicher (1984), the lack of red-displaced forbidden emission observed in many T Tauri stars indicates that an absorbing screen hides the receding part of the flow from our view. From the emission measure of observed lines, one can deduce that the minimum size of the screen must be on the order of 100 AU. Line profile computations by Edwards *et al.* (1987) suggest that a bipolar wind with latitude-dependent velocity best accounts for the detailed shapes of the lines.

As further indirect evidence for the presence of disks around T Tauri stars we show in this paper that the spectral energy distribution of many T Tauri stars can be reproduced over a large frequency range by assuming that the star is surrounded by an optically thick Keplerian accretion disk. Although this idea was first proposed by Lynden-Bell and Pringle (1974) in their classic paper on accretion disks, it had little impact on T Tauri research at that time, perhaps because the ultraviolet and infrared observations needed to fully test the model were not available.

Several groups have been independently reexamining the disk hypothesis for T Tauri stars in the last two years. Rucinski (1985) remarked that the spectral slope of T Tauri stars in the far-infrared *IRAS* range is in many cases close to that expected for an accretion disk, and Beall (1986) was apparently first to discuss what disk temperature gradient is most appropriate for reproducing the infrared energy distributions of the ρ Ophiuchi low-mass, pre-main-sequence stars observed and classified by Lada and Wilking (1984), but he does not present detailed models. Adams, Lada, and Shu (1987) suggest an evolutionary sequence based on the infrared energy distribution for these stars and assume that the spectrum originates from a "passive" disk (i.e., a disk which merely reprocesses the stellar light) and from an infalling, dusty envelope. Bertout (1987) noted that if T Tauri stars are surrounded by "active" accretion disks (i.e., disks with intrinsic luminosity) a boundary layer should exist between disk and T Tauri star, since the matter rotating at Keplerian velocities in the inner disk (typically 250 km s^{-1} ; cf. Bouvier *et al.* [1986] and Hartmann *et al.* [1986]). He also predicted, from a limited set of data, that the spectral contribution of the boundary layer could be used to understand the ultraviolet excess of T Tauri stars. In a recent work Adams, Lada, and Shu (1988) examine the case of T Tauri stars with flat infrared spectra, and conclude that active disks can reproduce these spectra provided their temperature

gradient is less steep than that of classical accretion disks. The same stars were also studied by Kenyon and Hartmann (1987), who instead favor a passive, flaring disk. They also discuss the possibility that extreme T Tauri spectra have a component from the boundary layer of an active disk.

This paper explores in more detail the accretion disk hypothesis for T Tauri stars, and focuses largely on the boundary layer's role in forming the strong ultraviolet excess that T Tauri stars display, together with their infrared excess, when they are compared to main-sequence stars of similar spectral types. These ultraviolet and infrared excesses vary greatly from star to star (cf. Rydgren *et al.* 1984), as do the optical line spectra, which can range from weak H α and Ca II H and K emission superposed on a normal photospheric spectrum in the "weak emission-line" T Tauri stars, to a pure emission spectrum with no visible photosphere in the "extreme" T Tauri stars. The majority of the class members' emission characteristics lie between these two extremes (see Cohen and Kuhi [1979] for statistics).

Attempts at understanding the spectra of T Tauri stars have been numerous (cf. Bertout 1984). The most successful hypothesis so far assumes that T Tauri activity is simply scaled-up solar-type activity, and is due to Herbig (1970). He suggested that a deep-lying chromosphere with continuum optical depth of 0.1 to 1 at the temperature minimum (compared to 10^{-3} in the Sun) might cause the emission line spectrum and the blue and UV excess continua; and quantitative investigations by Dumont *et al.* (1973), Cram (1979), and Calvet, Basri, and Kuhi (1984) confirmed the validity of this approach for T Tauri stars with low and moderate emission characteristics, which form the majority of the class. In this picture, the infrared excess observed in many T Tauri stars must be *independent* of the blue and ultraviolet excesses, and is usually attributed to thermal reemission of stellar photons by a dusty envelope (Mendoza 1968; Cohen and Kuhi 1979). The star is therefore the only source of photons in this view, and it must also power a wind with mass-loss rate typically of a few times $10^{-8} M_{\odot} \text{ yr}^{-1}$ (Kuhi 1964). Hence the "efficiency problem" discussed by DeCampli (1981). Although there has been some hope that Alfvén-wave driven winds could help solve this problem (Hartmann, Edwards, and Averett 1982), it is still uncertain whether dissipation of Alfvén waves can occur on a large enough scale to effectively accelerate the wind (cf. Holzer, Fla, and Leer 1983).

Another problem left unsolved by the classical approach is the ultimate origin of the energy flux necessary for forming the deep-lying chromosphere. While magnetism is often cited in this connection, it has become clear over the past two years that solar-type magnetic dynamo activity of T Tauri stars is by no means exceptional. Rotational modulation attributed to dark spots has been detected in several T Tauri stars, and the derived spot properties compare well with those found on RS CVn stars (Bouvier and Bertout 1987). The observed correlation between X-ray emission and rotation period also confirms the similarity of T Tauri and RS CVn classes as far as solar-type magnetic dynamo activity is concerned (Bouvier *et al.* 1985; Bouvier 1987). Although they are in different evolutionary stages, both classes of stars have similar rotation rates and deep convective layers, so that their similar degree of dynamo-driven activity is not entirely surprising. These results make it seem unlikely that magnetic dynamo activity *alone* can account for those properties of T Tauri stars which are not shared by the RS CVn stars. In particular, they make it now

difficult to believe that the deep-lying chromosphere of T Tauri stars can be formed directly by dissipation of magnetic waves originating in subphotospheric layers, given the sheer magnitude of the excess luminosity (comparable to L_{bol}) in some systems.

All the difficulties raised above about the energy balance of T Tauri stars are resolved if there is more than a single energy source in a typical T Tauri "system." We will demonstrate in the following that the accretion luminosity dissipated in an accretion disk and its boundary layer can account for up to a large fraction of the bolometric luminosity of T Tauri systems. Furthermore, the boundary layer has all the properties needed to create and maintain a chromospheric-like region in its vicinity. Another advantage of the accretion disk model is that the ultraviolet and infrared continua are correlated, so that only one physical mechanism—the presence of the disk interacting with the star—is needed to explain apparently unrelated phenomena.

The paper is organized as follows. The model is presented in § II, while § III is devoted to the description of our observational database. In § IV predicted disk colors are compared to observations, and models of individual stellar energy distributions are discussed in § V. Some further testable predictions of the disk models are contemplated in the final discussion.

II. DISK MODEL AND ITS EMITTED SPECTRUM

A typical T Tauri star is assumed here to be made up of a late-type star surrounded by an extended, thin accretion disk that reaches down to the stellar photosphere. Matter within the disk rotates with Keplerian velocities which are about 250 km s^{-1} just above the photosphere. As this matter is accreted onto the star, it must be slowed down to the photospheric rotation velocity in an equatorial boundary layer between disk and star. The quantitative model described below is a modification of the classical accretion disk model of Lynden-Bell and Pringle (1974; hereafter LBP), adapted to the particular case of T Tauri stars. It ignores the possible role of stellar magnetic fields on the structure of the disk and boundary layer, but plausible magnetic effects will be discussed qualitatively in § V. Following LBP we further assume that disk accretion proceeds in a steady-state when computing the temperature structure and emitted spectrum.

a) Accretion Disk

The temperature distribution in the disk is found by equating the rate of heating within a disk annulus of width dr located at radius r from the center to the radiated flux from both surfaces of the annulus. While we assume with LBP that the disk is viscous, Adams, Lada, and Shu (1987) have pointed out that the rate of energy dissipation per unit face disk area $F_{\nu}(r)$ does not depend on the origin of the dissipative torque which gives rise to angular momentum transfer within the disk. In the case of a Keplerian disk, and assuming that the central star rotates slowly, $F_{\nu}(r)$ is given by

$$F_{\nu}(r) = \frac{3GM_*\dot{M}}{8\pi r^3} \left[1 - \sqrt{\frac{R_*}{r}} \right], \quad (1)$$

where \dot{M} is the accretion rate through the disk, and where M_* and R_* are respectively the stellar mass and radius. By integrating $F_{\nu}(r)$ over the disk, one finds that half of the accretion luminosity

$$L_{\text{acc}} = \frac{GM_*\dot{M}}{R_*} \quad (2)$$

is radiated from the disk. We now include additional disk heating due to stellar light absorption, since it is of some importance for the energy balance in the disk's innermost regions (Friedjung 1985). The net effect of stellar light absorption by the disk is to convert 25% of the stellar luminosity into infrared photons. The absorbed stellar flux, again per unit disk face area, is found from geometrical arguments (cf. Adams and Shu 1986). It is

$$F_A(r) = \frac{\sigma}{\pi} T_{\text{eff}}^4 \left[\phi - \frac{\sin 2\phi}{2} \right], \quad (3)$$

where $\phi = \sin^{-1}(R_*/r)$ and where T_{eff} is the star's effective temperature. Assuming that the disk is optically thick (to be verified *a posteriori*), leads to a radial temperature distribution of

$$\sigma T_D^4(r) = F_{\nu}(r) + F_A(r). \quad (4)$$

The emitted disk spectrum can now be calculated assuming either that each annulus emits like a blackbody at temperature $T_D(r)$ or that each annulus emits the spectrum of a star with effective temperature $T_D(r)$. While the latter procedure should give better results, we cannot use it here because the temperatures of the disks surrounding T Tauri stars are too low (typically $T \leq 3000 \text{ K}$; see below). We therefore use the former approach here. We adopted Tylanda's (1977) formulation for shadowing of the boundary layer and extended it to the shadowing of the disk by the star. Shadowing of the star by the disk is easily computed.

Emitted flux from the disk at wavelength λ seen by an observer located at distance d and whose line of sight makes an angle i with the normal to the disk plane is then given by

$$F_{\lambda}^D = \left(\frac{2hc^2}{\lambda^5} \right) \left(\frac{R_*}{d} \right)^2 \cos i \int_1^{R_D/R_*} \frac{\pi + 2\gamma_0(x)}{e^{hc/\lambda k T_D(x)} - 1} x dx, \quad (5)$$

where $x = r/R_*$, where R_D is the disk's maximum radius, and where γ_0 , which takes shadowing by the star into account, is given by $\sin i \sin \gamma_0 = (1 - x^{-2})^{1/2}$ for $1 < x < 1/\cos i$, and by $\gamma_0 = \pi/2$ for $x > 1/\cos i$.

b) Boundary Layer

The second half of the accretion luminosity is emitted in the boundary layer where matter is accreted onto the star and where it presumably loses its kinetic energy in a series of weak oblique shocks. The dynamics of boundary layers are actually quite complicated, as hydrodynamic simulations show for white dwarfs (Robertson and Frank 1986; Kley and Hensler 1987). In the absence of detailed computations relevant to T Tauri stars, we have chosen to adopt here a simple approach. We assume that available energy is radiated away in an annulus of width δ which is characterized by a unique temperature T_{BL} given by

$$4\pi R_* \delta \sigma T_{\text{BL}}^4 = \frac{GM_*\dot{M}}{2R_*}. \quad (6)$$

Again, our assumption of a large optical thickness of the emitting region will be verified (§ II d).

The main parameter in equation (6) is the width δ over which emission from the boundary layer occurs. LBP and later Tylanda (1977) assume that it is equal to the size of the boundary layer itself, which depends on the viscosity. For the LBP viscosity prescription (see below), δ is equal to $10^{-2}R_*$. It is however more likely that emission from the boundary layer

occurs on a radial scale similar to the local height scale (Pringle 1977), which in turn depends on whether the boundary layer has time to expand before the heat generated inside it is radiated away. This question was investigated by Pringle and Savonije (1979) and Tytenda (1981). Both works support the view that δ is equal to the height scale of the disk just before entering the boundary layer. In other words, the radiative cooling time is always shorter than the adiabatic expansion time for the turbulent boundary layers of thin disks.

Assuming hydrostatic equilibrium in the vertical direction leads to a disk height scale of

$$h(r) = \sqrt{\frac{kT_D(r)}{G\mu m_H M_*}} r^{3/2}, \quad (7)$$

where μ is the mean molecular weight at r and where $T_D(r)$ is derived from equations (4). The width δ over which boundary layer emission occurs is assumed to be

$$\delta = h(R_* + \delta), \quad (8)$$

For computing μ , we assume that the disk is made up of H_2 , H_2^+ , H^- , H , H^+ , and electrons; and we solve the coupled system of statistical equilibrium equations with Vardya's (1961) equilibrium constants. Since μ is a function of T_D , an iterative procedure is used to solve equation (8); we find that δ is typically 2% of the stellar radius. The boundary layer flux is then

$$F_{\lambda}^{BL} = (\pi + 2\gamma_1) \frac{\delta}{R_*} \left(\frac{R_*}{d}\right)^2 \cos i B_{\lambda}(T_{BL}), \quad (9)$$

where γ_1 is found from

$$\sin \gamma_1 \sin i = \sqrt{1 - \left(\frac{R_*}{R_* + \delta/2}\right)^2}. \quad (10)$$

Notice that neither the disk nor the boundary layer spectrum depend on a given viscosity prescription. By choosing the disk height scale as the radial extent over which the boundary layer emits, we have replaced one assumption about the viscosity, which determines the radial scale of interaction between photosphere and disk (i.e., the boundary layer *dynamical* scale) with another physically more meaningful hypothesis about the size of the *radiative* region associated with that boundary layer.

c) Central Star

A common assumption that the central star radiates like a blackbody at the stellar effective temperature proved inappropriate for a study of the blue and ultraviolet excesses of late-type stars; line blanketing and ultraviolet chromospheric emission cause strong deviation from the blackbody curve in these spectral regions. We must therefore find a better description of the photospheric spectrum for actually comparing our models to observed T Tauri spectra.

If the interaction between the central star and its disk is confined to an equatorial boundary layer and has little effect on the *stellar* spectrum, one can approximate the emitted stellar spectrum by using a normal late-type spectrum. In our models, we used the energy distributions of either a normal late-type subgiant, or a chromospherically active pre-main-sequence star ("naked" T Tauri star; see § III for details about observations and data reduction methods), and we found that either assumption led to the same disk model when trying to reproduce a particular observed energy distribution. In other words, the chromospheric contribution to the blue and ultraviolet continua, if it is the same in "naked" and in "classical" T Tauri stars as arguments presented in §§ I and III suggest, is basically negligible in T Tauri stars with strong ultraviolet excess. Figure 1 displays three of our standard subgiant (*solid lines*) and naked T Tauri spectra (*dotted lines*). Blackbodies

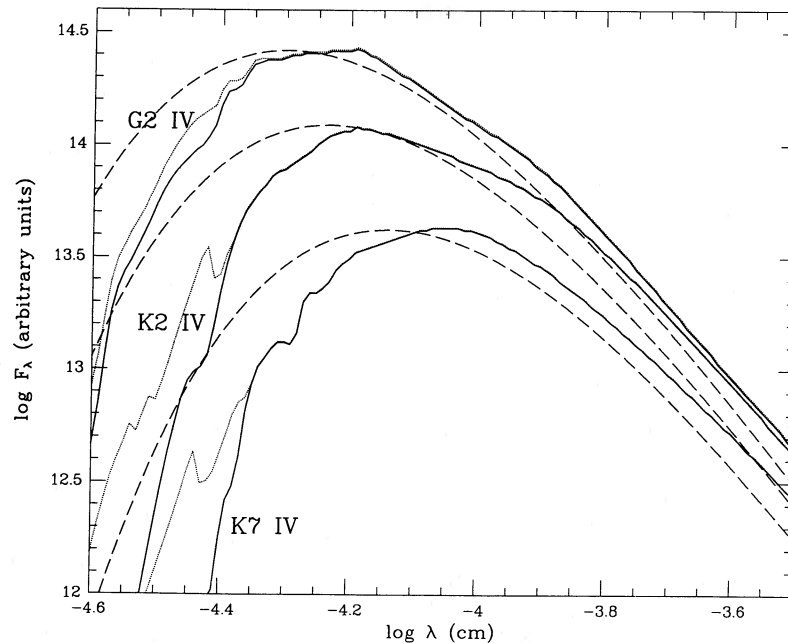


FIG. 1.—Stellar continuum distributions used to describe the underlying star. Three of the common spectral types are shown as labeled. The solid line is the photospheric contribution assembled from data on spectral standards (as described in § 3a). The dotted lines are the estimated average chromospheric contributions taken from data on a few naked T Tauri stars. The dashed lines are blackbodies with the effective temperature and bolometric luminosity of the photospheres, for comparison.

with the same effective temperature and luminosity (*broken lines*) are also shown for comparison.

The stellar contribution to the overall flux is then given by

$$F_{\lambda}^* = \frac{\pi}{2} (1 + \cos i) \left(\frac{R_*}{d} \right)^2 I_{\lambda}, \quad (11)$$

where I_{λ} is either a blackbody intensity at T_{eff} or a properly normalized stellar observed intensity.

The overall theoretical spectrum, found from equations (5), (9), and (11), is then reddened, using an observed A_V and the average extinction law given by Savage and Mathis (1979), in order to be compared to observed T Tauri spectral energy distributions. We also conducted tests using the HD 29747 extinction law advocated by Herbig and Goodrich (1986) for stars in the Taurus cloud, and found little difference in the derived disk properties. This is simply because the two extinction laws, which disagree widely in the short wavelength range of the *IUE* spectrograph, are not significantly different in the spectral ranges that we consider here (i.e., the *IUE* long wavelength range and redward). More specifically, differences between the two extinction curves can be compensated for by varying A_V within its associated error bars.

d) Optical Thickness of T Tauri disks

The assumption of large optical depth which was made above in the derivation of the disk's spectrum must now be examined. In a viscous disk, the equatorial disk surface density Σ is related to the energy dissipation rate $F_{\nu}(r)$ by (LBP):

$$F_{\nu}(r) = \frac{1}{2} \nu \Sigma \left(\frac{r d\Omega}{dr} \right)^2, \quad (12)$$

where ν is the gas viscosity and where Ω is the rotation rate. Using equation (1), we get

$$\Sigma = \frac{\dot{M}}{3\pi\nu} \left[1 - \left(\frac{R_*}{r} \right)^{1/2} \right]. \quad (13)$$

We then define an average gas density (in g cm^{-3}) by

$$\rho = \Sigma/2h \quad (14)$$

where h is computed from equation (7). Instead of using detailed gas opacity tables for computing the integrated optical depth, we adopt here the approximate analytic fits of Lin and Papaloizou (1985) to Rosseland opacities in the relevant temperature and density range.

Viscosity must now be dealt with, since it controls angular momentum and mass transfer in the disk, and hence its density. As discussed by Lin and Papaloizou (1985), the disk is probably convectively unstable in the vertical direction, which would induce turbulent motion. In this picture, the energy associated with the chaotic motion is transferred to smaller and smaller scales until the local viscous stress is sufficiently large for kinetic energy of the eddies to be dissipated into heat on an eddy turnover time scale, thus providing thermal energy to the disk. The release of gravitational energy in the accretion process compensates the gas kinetic energy loss.

In the absence of a definitive theory of turbulence-induced viscous dissipation, several parametrizations allowing for analytical solutions of the disk equations have been proposed for the viscosity. For example, LBP assume that the effective Reynolds number β^{-1} is constant throughout the disk, so that

$$\nu = \beta \Omega r^2. \quad (15)$$

LBP use $\beta = 10^{-3}$, the maximum laboratory flow value. Shakura and Sunyaev (1973) first proposed the now widely used α -prescription

$$\nu = \alpha c_s h, \quad (16)$$

where α is a scalar comparable to or less than 1 for transonic or subsonic turbulence, where c_s is the speed of sound, and where h is the disk height scale. This parametrization is useful because it relates ν in a plausible way to the local physical conditions in the disk. The relationship between these two prescriptions is given by

$$\alpha/\beta = (v_{\phi}/c_s)^2, \quad (17)$$

where v_{ϕ} is the rotational velocity.

We used both prescriptions to test our assumption about optical depth. Because rotational velocities are always highly supersonic in our models, there was little difference between the cases $\beta = 10^{-3}$ and $\alpha = 1$. The optical depth close to the star is sensitive to disk heating by the star (eq. [3]), which reduces the optical depth as H^- is depleted with increasing temperature. This is illustrated in Figure 2, where the optical depth of an "average" T Tauri disk model (Model B in Table 1) is plotted versus the disk radius for $\alpha = 1$, both with and without stellar light reprocessing in the disk, and then for $\beta = 10^{-3}$ with reprocessing (note that we have included a factor $\frac{2}{3}$ in the definition of ν for the sake of convenience). Figure 2 demonstrates that our "average" T Tauri disk model is indeed marginally optically thin in the range $1 < r/R_* < 1.15$, while the boundary layer remains optically thick. Computational tests have however shown that the region over which disk emission becomes thin is so small compared to the overall disk area that the spectrum is not appreciably altered even for a mass-accretion rate as low as $10^{-8} M_{\odot} \text{ yr}^{-1}$ (i.e., modifications of the emitted spectrum are lower or comparable to the accuracy of the photometric measurements). The optically thin region should however be taken into account in computations with lower mass-accretion rates, provided α is indeed of order unity. Lower α 's cause higher densities (and optical depths) for a given mass-accretion rate; but unfortunately, little is known about the magnitude of α except that it cannot be much higher than 1. We feel that there is little reason to introduce α as another free parameter of the computation at this stage of the investigation, and we therefore assumed an optically thick disk in the following (there is no need to choose an explicit value for α in that case).

Figure 2 also illustrates the main properties of optical depth variation with radius. Temperatures are very low (10–100 K) far away from the star ($r \gtrsim 10^{13}$ cm), so that ice grains contribute most to optical depth. At a radius of about 10^{13} cm, evaporation of ice mantles causes opacity to drop. At a radius of about 10^{12} cm, the kinetic temperature then reaches values

TABLE 1
PROPERTIES OF TYPICAL T TAURI DISKS^a

Parameter	A	B	C
\dot{M} ($M_{\odot} \text{ yr}^{-1}$)	4×10^{-7}	2×10^{-7}	1×10^{-7}
T_{BL} (K)	10500	8900	7500
δ/R_*	2×10^{-2}	2×10^{-2}	2×10^{-2}
L_{acc}/L_*	2.0	1.0	0.5

^a Parameters common to all three models: $M_* = 1 M_{\odot}$, $R_* = 3 R_{\odot}$, $T_{\text{eff}} = 4000$ K, $R_D = 10^3 R_*$.

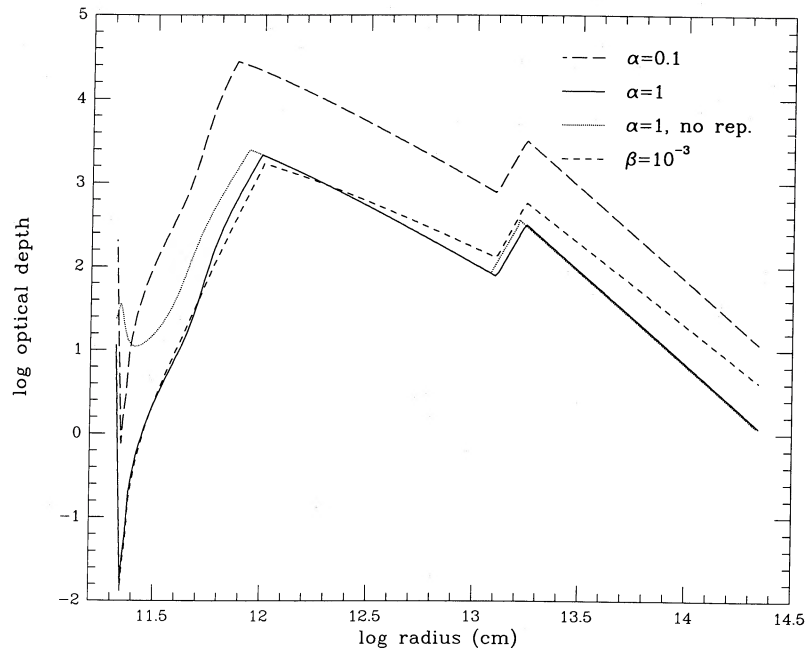


FIG. 2.—The Rosseland mean optical depth of the “average” disk model (model B) for various prescriptions of the viscosity, as a function of radius

high enough for the grains to be completely destroyed, and the opacity drops by several orders of magnitude. Finally, the spike at the stellar boundary is caused by the boundary layer, with a typical temperature of 10^4 K and with a high optical depth due mainly to bound-free and free-free hydrogen opacity.

e) Physical Properties of Disks and Role of Model Parameters

Figure 3 summarizes the main physical properties of disks representative of the T Tauri disks investigated in § IV, and Table 1 gives relevant numerical values for the mass-accretion rate \dot{M} , boundary layer temperature T_{BL} and thickness δ/R_* , and ratio of accretion to stellar luminosities L_{acc}/L_* . Panel (a) of Figure 3 shows the overall emitted spectra while the heavy dashed curve shows the contribution of a K7 photosphere (including chromospheric emission; see § III). Note the strong correlation between the magnitudes of the ultraviolet and near-infrared excesses in these spectra, computed for a view angle $i = 45^\circ$ and an visual extinction value of 1.0 mag. Panel (b) shows the variation of optical depth with radius, computed with $\alpha = 0.1$. Panel (c) illustrates the run of temperature with radius; at large distances from the star, T varies as $r^{-3/4}$. Finally, Panel (d) shows the variation of gas height scale with radius, which follows $r^{9/8}$ except in the inner regions where variation in molecular weight causes deviations from this power law.

There are six input parameters in our computations. They are the stellar spectral type and stellar radius R_* , the visual extinction to the system A_v , and the disk parameters \dot{M} , R_D , and i . We first show that four of these parameters can in fact be fixed independently by observational constraints, leaving us with only two adjustable parameters (\dot{M} and i) when fitting disk models to observed energy distributions of T Tauri stars. Then we show how these parameters affect the predicted energy distribution.

Figure 4a displays the respective contributions of the three system components (star, disk, and boundary layer) to the

overall spectrum for an “average” T Tauri disk (case B in Table 1). The stellar contribution (labeled “phot.”) dominates the spectrum in the optical range, so that, as observed, most T Tauri stars will exhibit classifiable photospheric spectra (see also the discussion of spectral veiling in § VI). Furthermore, we can determine both the stellar radius and the visual extinction in front of the system by requiring that the photosphere contributes most of the optical luminosity. This procedure, which works well for all T Tauri stars with visible photospheric spectra, allows one to derive the stellar radius to about 10% accuracy. The visual extinction is found to within about 0.2 mag by matching the red spectral region to that of a standard star with the same spectral type (see § III).

The effect of varying disk maximum radius R_D on the far-infrared part of the spectrum is illustrated in Figure 4b. In our actual computations, this parameter was kept constant and equal to $10^3 R_*$, resulting in the constant spectral slope characteristic of disks, $\lambda F_\lambda \propto \lambda^{-4/3}$, over the entire far-infrared range. We are thus left with two parameters, the mass-accretion rate \dot{M} and the view angle i .

Figure 4c demonstrates that an accurate extinction determination is of importance in order to study the contribution of the boundary layer to the spectrum. Because of (i) the sensitivity of the ultraviolet spectrum to the adopted extinction value and (ii) the rapid light variations in the UV and blue ranges observed in many T Tauri stars, we believe that *nearly simultaneous ultraviolet and optical flux measurements are necessary in order to estimate the mass-accretion rate and accretion luminosity*. Even when such measurements are available, these estimates could still be affected by assumptions on the extinction law. As mentioned earlier, we use the average extinction law of Savage and Mathis (1979) throughout this work, but tests with the HD 29747 extinction of Herbig and Goodrich (1986) yield no appreciable changes in the derived model parameters.

The effect of the two main parameters on the computed spectral energy distributions is also illustrated in Figures 3 and

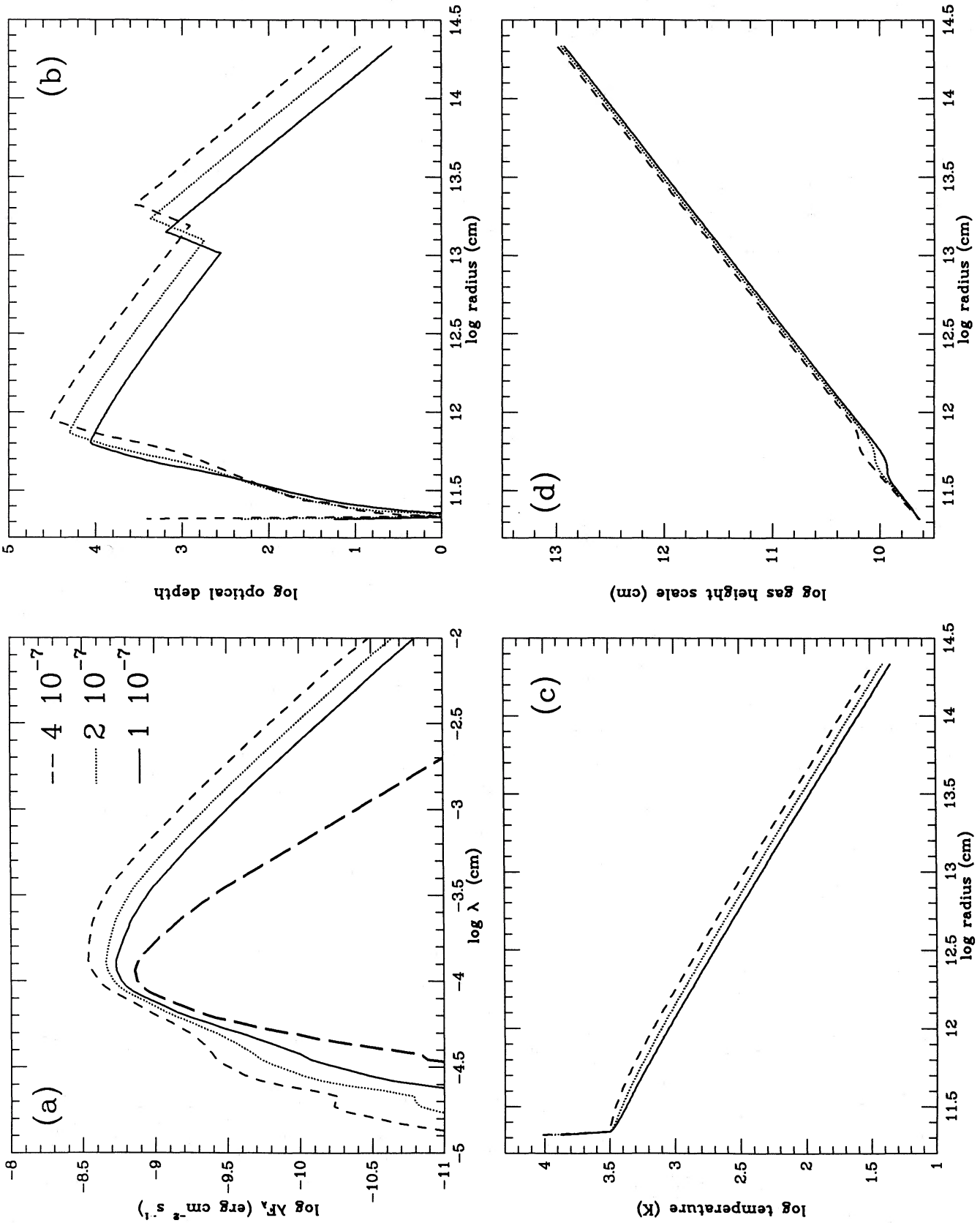


FIG. 3.—Properties of typical T Tauri disks. (a) The emergent spectrum of disk plus boundary layer for models A, B, C (Table 1). The lower heavy dashed line shows the stellar photosphere for the assumed K7 underlying star. (b) The optical depth through the disks as a function of radius. (c) The radial temperature distributions in the disks. (d) The gas height scale of the disks as a function of radius.

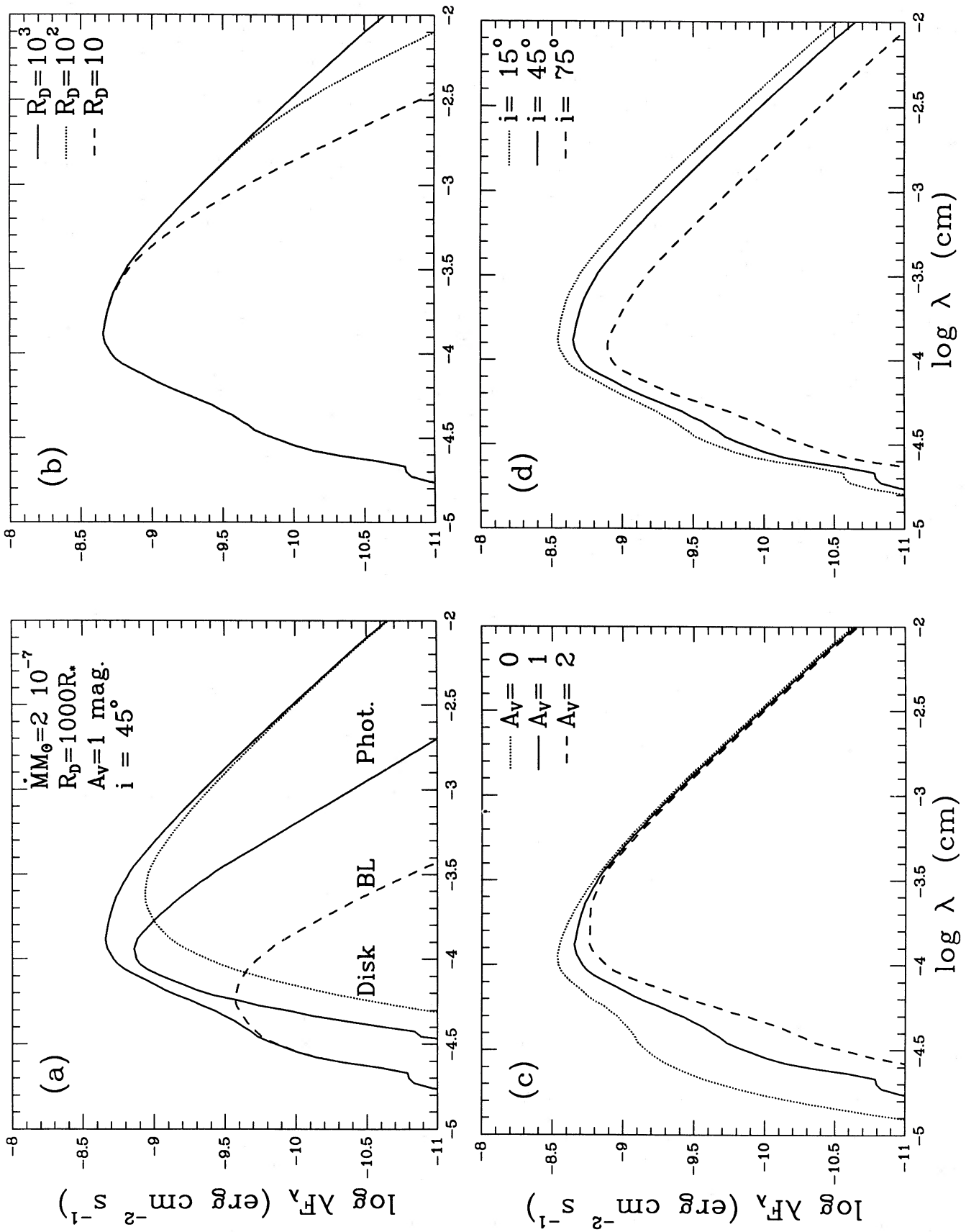


FIG. 4.—Physical contributions to the emergent spectrum. (a) The main physical components which make the systemic spectrum are shown individually. The K7 star is labeled "Phot." The boundary layer is labeled "BL." The disk itself is shown as a dotted line. (b) The effect of varying the disk radius is shown. (c) The effect of extinction on the emergent spectrum. (d) The effect of the inclination of the disk.

4. Increasing the view angle i lowers the observed flux without basically altering the overall spectral shape (Fig. 4d). The effect of increasing \dot{M} , shown in Figure 3a, is to increase both infrared and ultraviolet excesses with respect to the photospheric contribution.

Actually, the main parameter in the computation is not \dot{M} alone, as was implied above, but rather the combination $\dot{M}M_*/R_*^3$, which determines both the disk temperature distribution (cf. eq. [1]) and, together with δ/R_* , the boundary layer temperature (cf. eq. [6]). We have considered in our discussion above that R_* was independently known with a high enough accuracy that it could be considered constant. While this is true for many of the stars we investigate, it is not true for the most extreme T Tauri stars, i.e., those stars which exhibit no photospheric spectrum. For these stars, the photospheric parameters are thus adjustable, and the derived disk models are therefore somewhat more arbitrary. It is however worth emphasizing that less than 10% of the T Tauri stars are that extreme. In the large majority of cases, the photospheric spectrum is indeed visible, so that only two free parameters, \dot{M} and i , are available to model the observed spectra.

III. OBSERVATIONS

a) Spectrophotometry

Because of the rapid and sometimes large variability of the T Tauri stars, particularly at shorter wavelengths, it is very desirable to have observations over the entire wavelength region of interest obtained at the same time. As emphasized in the last section, it is optimal to include the spectral range from the vacuum ultraviolet to the mid-infrared. Of course it is difficult to obtain such observations, as they require at least three different types of instrumentation, one of which must be in orbit! Fortunately it has been clear that simultaneous UV and optical observations would be a valuable diagnostic tool well before specific disk models were considered. We have been conducting a program to gather *IUE* and optical spectra at nearly the same time in 1980, 1983, and 1985 for a total of 17 stars. Some results from these are discussed in Calvet *et al.* (1985) and in Basri, Finkenzeller, and Imhoff (1988). These papers concentrate on measurements of emission-line fluxes

but because the observations were spectrophotometric they are also useful in the context of testing continuum distributions predicted by disk models. Since the predicted peak of the boundary layer emission is in the UV, with a much subtler impact in the optical (for lower accretion rates), such observations are in fact the primary tool required for studying accretion in young stars.

The 14 stars selected for study in this paper are summarized with a few relevant observational properties in Table 2. Since the observations have been discussed at length in the above papers, we do not repeat detailed observing logs here. In all cases we have restricted ourselves to long wavelength camera observations with *IUE* since stellar continuum is rarely observed in the short wavelength range for T Tauri stars. Even between 2000 and 3000 Å it is not clear whether one is observing true continuum or an "emission-line haze" at low dispersion, and the spectra tend to be rather noisy. We have taken a trend line through the middle of the data in most cases; this is likely to be an upper limit to the actual continuum radiation from the star. Obvious emission features were avoided. The data were averaged over 50 Å bandpasses and fitted with a smooth curve to generate the observational points plotted in later figures.

The optical observations were all made with the IDS on the 1 m Nickel telescope at the Lick Observatory. The spectral range covered only from the Ca II K line to H β for the 1980 data, but ran from the K line to the infrared triplet of Ca II in the 1983 and 1985 data. The observations were typically gathered over a few days contemporaneous with an *IUE* run, but are not strictly simultaneous. For stars with strong rotational modulation or flaring this could cause some error in the comparison of UV and optical, but these variations are generally smaller than in the more long-term trends seen in T Tauri stars.

The spectral types from Cohen and Kuhi (1979) were checked against our own spectral standards and found to be generally satisfactory. It is very helpful that the deep photospheres of T Tauri stars look normal—as confirmed by Finkenzeller and Basri (1987) from the line spectra—since we can proceed to construct the continuum distributions expected for the star without a disk. We used a combination of the Jacoby,

TABLE 2
OBSERVATIONAL DATA

Star	Sp. Type ^a	A_V^a (mag)	L_{bol}/L_{\odot} (0.36 μm –100 μm)	$v \sin i$ (km s ⁻¹)	P_{rot}^b (days)
V140 Tau	K4	0.0	2.0	73.5 \pm 10.5 ^c	1.95
BP Tau	K7	0.55 \pm 0.3	1.6	<10 ^d	...
DE Tau	M1	0.2 \pm 0.02	...	<10 ^d	...
RY Tau	K1	1.0 \pm 0.2 ^e	21.8
T Tau	K1	1.0 \pm 0.2 ^e	21.6	19.5 \pm 2.5 ^b	2.8 ^f
DF Tau	M0.5	1.6 \pm 0.6 ^e	3.5	21.6 \pm 9.2 ^b	8.5
DG Tau	G? ^h	...	7.9
UX Tau A	K2	0.2 \pm 0.04	2.1	27.0 \pm 2.0 ^b	2.7
GG Tau	K7-M0	1.0 \pm 0.3 ^e	2.3	<10 ^d	...
DN Tau	M0	0.42 \pm 0.16	0.9	8.1 \pm 2.0 ^b	6.0
DR Tau	K5? ^g	...	5.1
DS Tau	K3	0.33 \pm 0.32	0.75	<10 ^d	...
SU Aur	G2	0.93 \pm 0.14	10.0	66.1 \pm 15.8 ^b	...
RW Aur	K2? ^h	...	4.6	19.5 \pm 4.6 ^d	...

^a Cohen and Kuhi 1979.

^b Bouvier *et al.* 1986.

^c Vogel and Kuhi 1981.

^d Hartmann *et al.* 1986.

^e This work.

^f Herbst *et al.* 1986.

^g Joy 1949.

^h Mundt and Giampapa 1982.

Hunter, and Christian (1984) and *IUE* (Wu *et al.* 1983) spectral atlases to construct the continuum distribution for normal stellar photospheres that appear in Figure 1. Note that these depart from an equivalent blackbody distribution especially in the ultraviolet. This is of course because the continuum forms at smaller depths (and therefore temperatures) as the opacity increases in the ultraviolet.

Next we consider what the distribution of infrared continuum light from the star alone is. Although this may seem a trivial task, good compilations of IR colors out to 10 μm for cool subgiant photospheres are not available. The usual assumption is to take a blackbody at the effective temperature but as in the rest of the spectrum this is not accurate since the IR continuum is formed a little deeper and hotter than the level at which the photospheric temperature equals the effective temperature. We collected colors for normal stars of the appropriate temperature and luminosity from the compilation of Johnson *et al.* (1966). These gave fairly consistent measures of the slope of the infrared continuum relative to the optical spectrum and have also been incorporated into Figure 1. Thus for each of the spectral types for which we have T Tauri observations, we have attempted to define the continuum distribution which arises from the active star alone. Any further excess must then be ascribed to material off the star.

The issue of extinction is fairly critical for the disk analysis and so will bear further study. The detailed spectral type and luminosity class of a standard star used to find extinction has an uncomfortably sensitive impact on the value obtained. We found, for example, that the spectrophotometry of T Tauri was best fitted with an extinction of 1.0 mag using a K0 V standard and even less using a K2 V standard. The value of 1.4 given in the literature was most closely matched if we used giants as standards. For the future, the best procedure will be to collect spectrophotometry for a grid of naked T Tauri stars which can be used to more carefully determine the extinction in the stars with disks. Walter (1987) finds, however, that the colors of these stars are very nearly those of main-sequence stars of the same spectral types. Since this is essentially the assumption Cohen and Kuhl were making, we do not expect their values to be grossly in error for stars in which the spectral type is clear.

Even the naked T Tauri stars exhibit strong chromospheric activity which could in principle give rise to a UV excess via chromospheric continuum emission as shown by Calvet, Basri, and Kuhl (1984). We looked in detail at the UV excess in a few stars for which there is no obvious IR excess and small H α equivalent widths. In particular, we had optical and UV data for five such cases: UX Tau and Sz 68 (K2), V410 Tau and Sz 65 (K7), and Sz 82 (M0). For each (dereddened) star we subtracted a photospheric contribution derived from our spectral standards, with all spectra normalized at 7000 \AA . We then integrated the remaining flux in the wavelength range from 2600 \AA to 3000 \AA , excluding the Mg II emission. The resulting absolute energies were in the ratios 1.9:2.4:1.4:1.0:1.1 (in the same order as listed above). When normalized by the flux in Mg II they were all approximately the same. Thus, these stars have remarkably similar amounts of UV light in excess of what is expected for the photospheric spectral type. The chromospheric strengths are actually slightly different, but this shows up in both the UV excess and the measured Mg II strengths.

Although it is tempting to scale the UV excess by the Mg II emission for all the stars, we believe this would not be a good idea because boundary layer and wind emission very likely contribute to Mg II in the more active stars (Calvet *et al.* 1985),

as is also implied by the nonchromospheric character of the Mg II profiles in the stars with disks. Any scaling from line fluxes must be done from high-resolution observations in which it is clear that a purely chromospheric (narrow, symmetric) profile has been measured. An example of the Ca II lines showing both a chromospheric component and a much broader component was presented by Basri (1987) for BP Tau; GG Tau has also this characteristic. Another argument that the intrinsic chromospheric strength is similar in the absence of a disk can be found from a comparison of the emission-line strengths in the naked stars (Basri, Finkenzeller, and Imhoff 1988), which are all rather similar and lie between active main-sequence stars and the T Tauri stars with evidence for disks and winds.

The fact that the naked star chromospheres are so similar across the range of spectral types gives us some confidence that we can assess the level of the chromospheric contribution to the UV excess. We used the average level of the excess UV continuum for the five stars above and added it to our standard photospheres to yield "chromospheric standards" as shown in Figure 1. It is these spectral distributions which are used as the stellar contributions in the subsequent boundary layer modeling. We believe that the chromospheric levels we have determined from the stars without infrared excesses yield fairly reasonable estimates of the UV excess that arises unambiguously from classical stellar chromospheres. It is possible that in a few cases the chromospheres are actually a little stronger than those implied here, but so far there is no evidence that the large excesses observed in some of the classical T Tauri stars are ever observed in stars without disks. In order to generate such excesses in classical stellar chromospheres, a significant fraction of the stellar bolometric luminosity would have to be dissipated as nonradiative energy immediately above the photosphere. We know of no way to accomplish this, so the cases discussed by Calvet, Basri, and Kuhl (1984) remain purely hypothetical.

Finally, we have begun to collect spectra between the region of the K line (about 4000 \AA) where most of our optical observations ended and the excess was still mild, and the *IUE* spectral range where the excess is already quite strong. While the study of the spectra in this range is worthy of a separate paper (in preparation) we thought it worthwhile to anticipate a few results in the context of this work (see also § V). Briefly, it appears that many of the active stars achieve their excess as a strong Balmer continuum emission jump (as shown for BP Tau and GG Tau below). There are notable exceptions to the general prevalence of Balmer jumps; for example, RW Aur and RY Tau show little change across the jump. We have arbitrarily included a modest jump in our "standard chromosphere" spectrum (despite its absence in any naked star spectrum), but it has no real effect on the cases in which there is clearly a boundary layer (because it is swamped by the boundary layer emission).

b) Optical and Infrared Photometry

The nearly simultaneous optical and infrared photometric data used in this investigation were also gathered with other motivations in mind, specifically for studying the stellar light curves on a day-to-day basis. The full set of data will be published separately (Bouvier, Bertout, and Bouchet 1988), so we need only give a summary of observational procedures

here. These observations were not at the same time as the optical-ultraviolet studies discussed above.

UBVRI photometry was done from 1984 December 9 to December 21, with the standard set of Cousins filters at the 50 cm ESO telescope equipped with a cooled RCA 31034 Quantacon photomultiplier tube. Typical integration time was 1 minute followed by a 20 s, integration on the sky. Around 20 Cousins photometric standards taken from Graham (1982) have been measured each night in order to get the final colors in the standard *UBVRI* Cousins system (Bessel 1979). Furthermore, comparison stars near the targets of similar spectral type and magnitude were observed. They were later used to check the stability of the system during the night and the consistency of the reduction process from night to night. Weather conditions during the observing run were photometric except for the sixth night during which cirrus appeared. Typical uncertainties on the individual measurements are on the order of 0.02 mag in the *B* through *R* bands, and 0.05 to 0.1 mag in the *U* band, depending on the faintness of the target stars in this band.

JHKL photometry was performed by P. Bouchet from 1984 December 15 to December 21 using the ESO infrared photometer/spectrophotometer attached to the 1 m ESO telescope. The photometer is equipped with a InSb detector cooled at 77 K, and the filters match Johnson's standard broad-band photometric system (Johnson 1964). The stars were observed through a 15" diaphragm, and sky subtraction was achieved by chopping at 7 Hz frequency in the east-west direction with a throw of 20" amplitude, and by beam-switching. Typical integration times were 2 minutes for each of the *J*, *H*, and *K* filters, and 3 minutes for *L*. Photometric standards from Koornneef (1983) were measured each night to determine the atmospheric extinction. Final color transformations to Johnson's system and zero-point determinations were performed by gathering all standard star measurements over the observing run. The final error bars, about 0.05 mag in filters *J* through *K* and 0.1 mag in *L*, take into account errors in the measurement and extinction coefficient as well as uncertainties arising from the color transformations and zero-point determinations.

c) Additional Data

The objects common to the two sets of data discussed above are: V410 Tau, BP Tau, RY Tau, T Tau, DF Tau, DG Tau, UX Tau A, DN Tau, and SU Aur. In addition, spectrophotometric *IUE* and optical data are available for DE Tau, DR

Tau, DS Tau, GG Tau, and RW Aur, and we averaged the nonsimultaneous broad-band photometric data from the compilation by Rydgren *et al.* (1984) to supplement our data base for these objects. Herbig and Goodrich (1986) published near-simultaneous *IUE* and optical data for V410 Tau, T Tau, and DR Tau, and we also used them together with our own data in order to get some idea of the flux variability on time scales of years. Finally, the far-infrared data are from the *IRAS* Point Source Catalog, as compiled by Rucinski (1986). No attempt was made to color-correct the *IRAS* data, since this correction is usually quite small.

IV. THE COLORS OF DISKS

Before comparing detailed spectral energy distributions of disk models and stellar observations (§ V), we will compare predicted and observed color-color diagrams of T Tauri stars. Here, we focus on $(U-B)$ versus $(K-L)$, which measures the correlation between boundary layer and disk emission, and $(U-B)$ versus $(B-V)$, because the disk hypothesis allows us to understand some of the peculiarities of this diagram.

a) $(U-B)_0$ versus $(K-L)_0$

Figure 5a shows theoretical disk colors computed with the disk model described in § II and observed colors of the 14 T Tauri stars in our data base. The filled squares are the averaged colors of these stars, corrected for the extinction value given in Table 2, and the bars indicate the standard deviation of the measurements over the observing period. Rather than indicate the star's names in this already crowded graph, we give in Table 3 the extinction corrected colors for all stars. Extinction values for the three extreme stars in our sample (DG Tau, DR Tau, RW Aur) are derived from the models of § V.

The open symbols display the theoretical disk colors for various mass accretion rates and disk view angles. We show two families of models computed for two different central stars; first, a $0.5 M_{\odot}$ M0 IV star with $3 R_{\odot}$ radius, labeled "M0"; and second, a $2 M_{\odot}$ K0 IV star with the same radius, labeled "K0". Squares stand for a view angle of 0° (pole-on view), circles for $i = 45^{\circ}$, and triangles for $i = 80^{\circ}$. Dotted lines connect the colors of the naked photosphere to colors computed for disk models with a same view angle but five equally spaced values of the parameter MM_* between 5×10^{-8} and $5 \times 10^{-7} M_{\odot}^2 \text{ yr}^{-1}$.

The effect of disk and boundary layer on the observed colors

TABLE 3
INTRINSIC COLOURS OF PROGRAM STARS^a

Star	$(U-B)_0$	$(B-V)_0$	$(V-R)_0$	$(V-I)_0$	$(J-H)_0$	$(H-K)_0$	$(K-L)_0$
V410 Tau	0.92	1.19	0.71	1.44	0.75	0.17	0.08
BP Tau	-0.14	0.93	0.72	1.50	0.85	0.38	0.64
DE Tau	-0.25	1.29	1.02	2.20	0.87	0.52	0.99
RY Tau	0.24	0.67	0.40	0.85	1.15	1.06	1.14
T Tau	0.28	0.87	0.49	0.92	0.87	0.63	1.11
DF Tau	-0.44	0.81	0.64	1.58	0.90	0.46	0.71
DG Tau	-0.37	1.14	0.93	1.93	1.12	0.96	1.73
UX Tau A	0.50	0.94	0.54	1.08	0.64
GG Tau	-0.26	1.05	0.73	1.39	0.90	0.40	0.79
DN Tau	0.66	1.29	0.83	1.72	0.83	0.33	0.42
DR Tau	-1.08	0.09	0.19	0.36	0.98	0.92	1.20
DS Tau	-0.28	0.83	0.65	1.26	0.80	0.41	0.63
SU Aur	0.28	0.75	0.42	0.82	0.67	0.44	0.72
RW Aur	-0.43	0.36	0.29	0.64	0.80	0.63	0.97

^a Colors corrected by observed (when available) or derived extinction values.

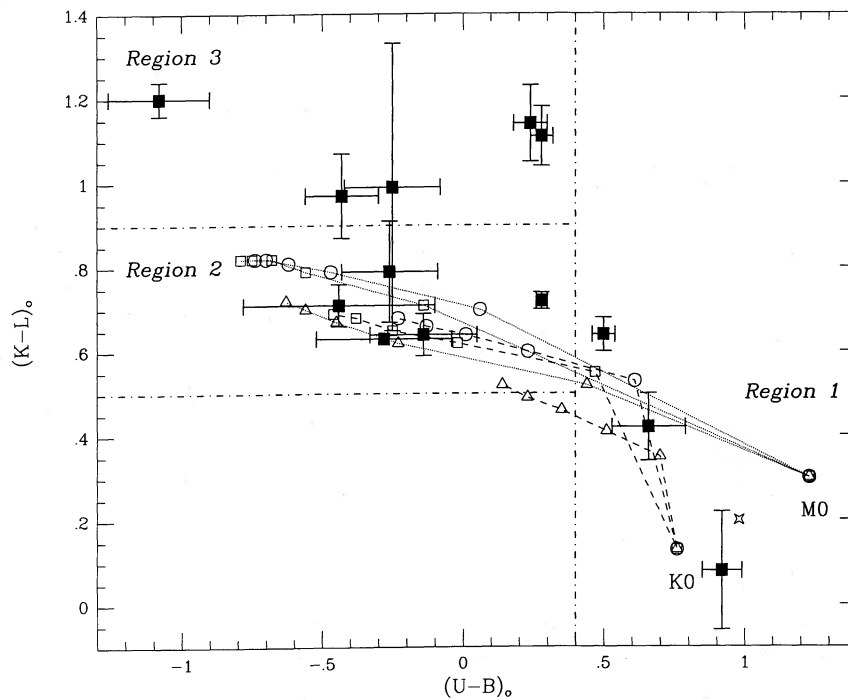


FIG. 5a

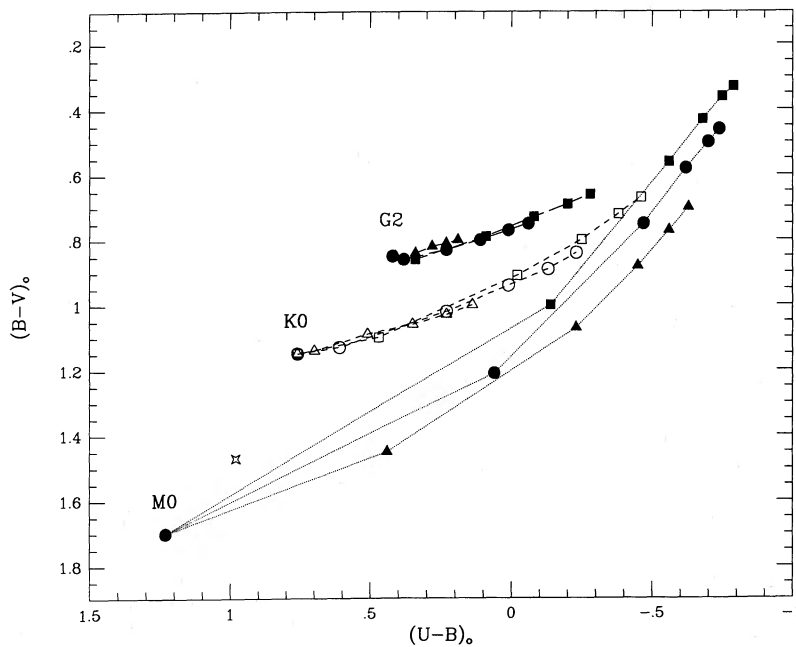


FIG. 5b

FIG. 5.—Color-color analysis of disks. (a) The $(U-B)-(K-L)$ plane. Both models and observations are shown here. The open symbols display the theoretical disk colors for various mass accretion rates and disk view angles. We show two families of models computed for two different central stars; first, a $0.5 M_{\odot}$ M0 IV star with $3 R_{\odot}$ radius, labeled “M0”; and second, a $2 M_{\odot}$ K0 IV star with the same radius, labeled “K0.” Squares stand for a view angle of 0° (pole-on view), circles for $i = 45^{\circ}$, and triangles for $i = 80^{\circ}$. Dotted lines connect the colors of the naked photosphere to colors computed for disk models with a same view angle but five equally spaced values of the parameter $\dot{M} M_{*}$ between 5×10^{-8} and $5 \times 10^{-7} M_{\odot}^2 \text{ yr}^{-1}$. The starred symbol between the two photospheres represents the colors of the K0 photosphere affected by 1 mag of visual extinction. The observational means and variations are shown with the filled squares and error bars. (b) The $(U-B)-(B-V)$ plane. Symbols are as above, with the addition of a G2 family of models.

is quite different for an M0 and a K0 photosphere. Adding an accretion disk to an M0 star results in a $U - B$ decrease of 1.2 mag for the smallest accretion rate considered here. But $U - B$ decreases only by 0.2 mag for the K0 star, because the contrast between boundary layer and photospheric emission is much higher for the cool M star. The $K - L$ increase of about 0.5 mag for the smallest accretion rate is the same for both cases because both photospheres have similar slopes in that spectral region. Notice that $K - L$ stays approximately constant when \dot{M} increases, while $U - B$ decreases to -0.9 mag for the M0 photosphere and for the highest mass accretion rate considered here.

Comparing the theoretical and observed colors, we see that the disk model can account for the entire range of observed $U - B$ values, but cannot explain the entire $K - L$ range. More precisely, the diagram reveals the existence of three groups of stars with quite different properties. The three stars with $(U - B)_0 \geq 0.5$ and $(K - L)_0 \leq 0.6$ (Region I), while not entirely "pure" photospheres, have $\dot{M} M_* \leq 5 \times 10^{-8} M_\odot^2 \text{ yr}^{-1}$ if they are at all surrounded by disks. They have, most likely, already accreted most of their disk. This first group consists of V410 Tau, DN Tau, and UX Tau A. The second group of stars, with $-1 \leq (U - B)_0 \leq 0.5$ and $0.6 \leq (K - L)_0 \leq 0.9$ (Region II) includes BP Tau, DF Tau, GG Tau, DS Tau, SU Aur, and (marginally) DE Tau; obviously, the accretion disk model is successful for these objects. Finally, a last group of stars with $(K - L)_0 \geq 0.9$ (Region III) includes the three extreme T Tauri stars DG Tau, DR Tau, and RW Aur as well as T Tau and RY Tau. We shall see below that the spectra of both DR Tau and RW Aur can be reproduced in the framework of a slightly modified disk model. The three remaining objects are the stars with flat far-infrared spectra discussed by Adams, Lada, and Shu (1988), and the classical accretion disk model does not allow us to reproduce their whole energy distribution.

b) $(U - B)_0$ versus $(B - V)_0$

The presence of disks around T Tauri stars may also help us understand their $(U - B)_0$ versus $(B - V)_0$ diagram. Mundt and Bastian (1979) noticed that T Tauri stars seem to gather in two separate regions of the $(U - B)_0 - (B - V)_0$ plane, one with $(U - B)_0 \leq 0$ and the other with $(U - B)_0 \geq 0$ (see their Figs. 1 and 2). Figure 5b displays the theoretical $(U - B)_0$ and $(B - V)_0$ disk colors. Symbols are as in Figure 5a, with addition of another family of models for a G2 photosphere.

We have noted earlier that the effect of the boundary layer on the $U - B$ color of a late-type photosphere is dramatic, since $(U - B)_0$ becomes negative for mass-accretion rates as low as $6-7 \times 10^{-8} M_\odot^2 \text{ yr}^{-1}$. Late-type photospheres [with $(U - B)_0 \geq 1$] and stars with even modest accretion disks and $(U - B)_0 \leq 0$ will therefore tend to be located in different regions of the diagram. This distinction vanishes for stars earlier than about K2 because the contrast between photospheres with and without boundary layers becomes smaller. Within the disk hypothesis, the separation of the stars into two groups noted by Mundt and Bastian (1979) thus occurs merely because a large majority of T Tauri stars have late-type photospheres, in complete agreement with the statistics of Cohen and Kuhl (1979) for stars in the Taurus-Auriga and Ophiuchus clouds. Orion T Tauri stars have somewhat earlier types, so we do not expect the separation to be as well defined; and this may well explain why the gap around $(U - B)_0$ is not as pronounced in Figure 1 of Mundt and Bastian's paper, which contains stars from several regions including Orion, as in their

Figure 2 which contains only stars from the Taurus-Auriga region.

V. ENERGY DISTRIBUTIONS OF INDIVIDUAL STARS

The basic strategy for making detailed models of stellar energy distributions follows. We compute a first model for the overall energy distribution using the stellar parameters derived from the optical observations and typical disk parameters. We then fine-tune the two main parameters (view angle and mass-accretion rate) until a reasonable fit of the data is reached over the largest possible wavelength range. A basic bias in our procedure is that we always maximize the photospheric contribution in the optical and near-infrared ranges; we thus use the largest possible stellar radius, and try to minimize veiling, the magnitude of which provides an additional constraint for our models (see also § VIb). Other observational constraints are discussed in the individual analysis. From the preceding section, we know that there are three subgroups of stars with quite different properties in our sample. The first one is that of stars with $(K - L)_0 \leq 0.6$ and $(U - B)_0 \geq 0.5$, which includes V410 Tauri, UX Tauri A, and DN Tauri. We do not expect these objects to be surrounded by optically thick, extended disks, and we do not study them further here. The two other groups of stars are discussed below, and their observed energy distributions are displayed together with computed disk spectra in Figures 6 to 9.

a) Stars with $0.6 \leq (K - L)_0 \leq 0.9$

This is the subgroup of stars best described by classical accretion disks. It comprises BP Tau, DE Tau, DF Tau, GG Tau, DS Tau, and SU Aur. The energy curves of these objects are discussed below, except for DF Tauri's, which displays particularly interesting properties and is discussed separately in § Vd, and DE Tauri's, a M1-M3 star for which we had no photospheric standard. The predicted and observed spectra of individual stars are presented in Figures 6 and 7, and the model parameters are given in Table 4a.

Figure 6 displays sample spectra of BP Tauri and GG Tauri over the 2300-9000 Å range. There, the extinction-corrected

TABLE 4A
MODEL PARAMETERS FOR OBJECTS WITH $(K - L)_0 < 0.9$

Star	Sp. Type	A_v	R_*/R_\odot	$\dot{M}/M_\odot \text{ yr}^{-1}$	M_*/M_\odot	i°
BP Tau	K7	0.4	3.0	2×10^{-7}	0.8	80
DF Tau	M0	1.2	3.8	3.5×10^{-7} $6.5^a \times 10^{-7}$	0.8	65
GG Tau	K7	1.1	3.5	4×10^{-7}	0.8	75
DS Tau	K4	0.6	1.8	6.5×10^{-8}	1.0	75
SU Aur	G2	0.45	3.1	6×10^{-8}	2.0	40

^a Models for two different epochs.

TABLE 4B
MODEL PARAMETERS FOR OBJECTS WITH $(K - L)_0 > 0.9$

Star	Sp. Type	A_v	R_*/R_\odot	\dot{M}/M_\odot	M_*/M_\odot	i°
RY Tau	K0	1.1	2.7	7.5×10^{-8}	2	55
T Tau	K0	1.0	3.4	1.1×10^{-7}	2	15
DR Tau	K4	1.8	1.2 ^a	5.0×10^{-7}	1	<10
RW Aur	K0	1.0	2.0 ^a	2.0×10^{-7}	1	<10

^a Inner disk radius is $3.5 R_\odot$ for DR Tau and $3.3 R_\odot$ for RW Aur.

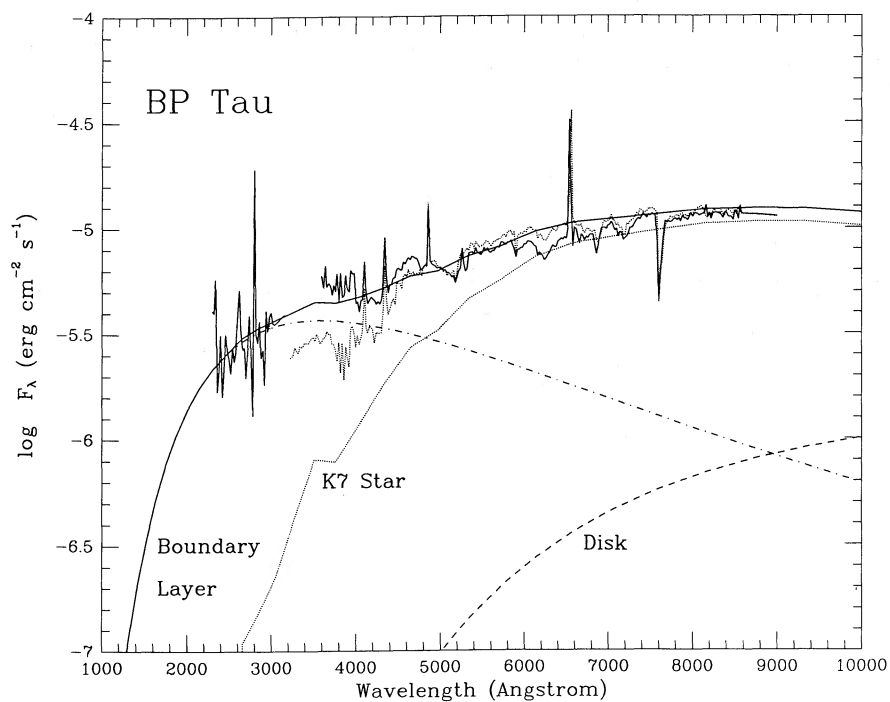


FIG. 6a

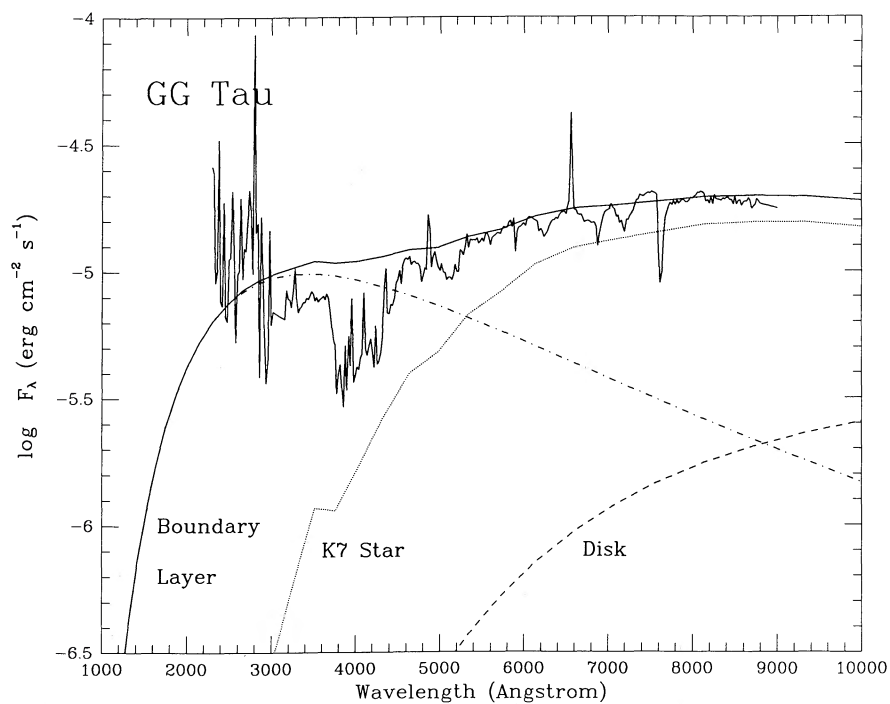


FIG. 6b

FIG. 6.—The optical and UV dereddened spectra of BP Tau and GG Tau. Both models and observations are shown. The total calculated systemic spectrum is the solid smooth curve, while the *photospheric plus chromospheric* stellar continuum is the dotted curve. The boundary layer (*dot-dashed*) and disk (*dashed*) contributions are also shown, along with observations dereddened by 1.1 mag for GG Tau and 0.4 mag for BP Tau. The observations consist of concurrent 1983 UV and optical spectra (*solid line*) with more recent optical data (1986 Oct; *dotted line*) from Balmer continuum region superposed.

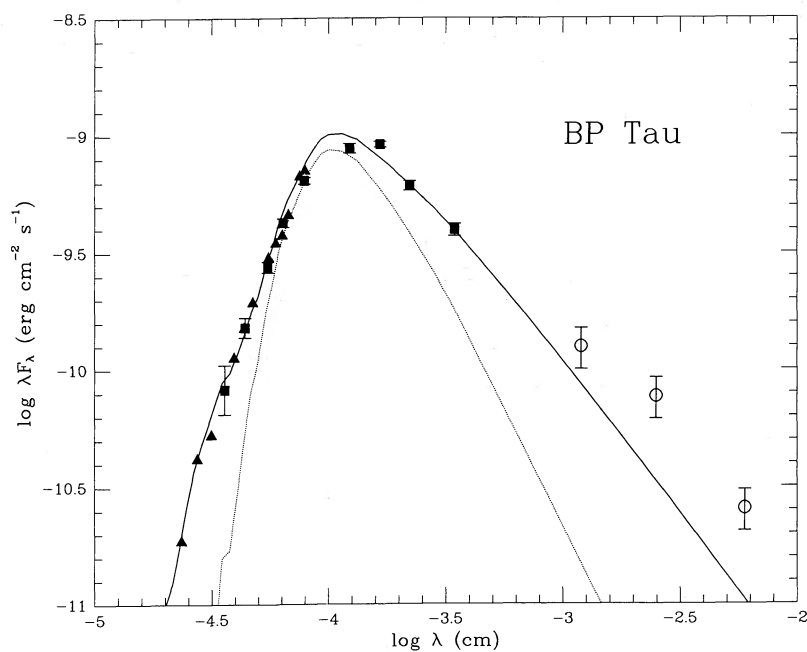


FIG. 7a

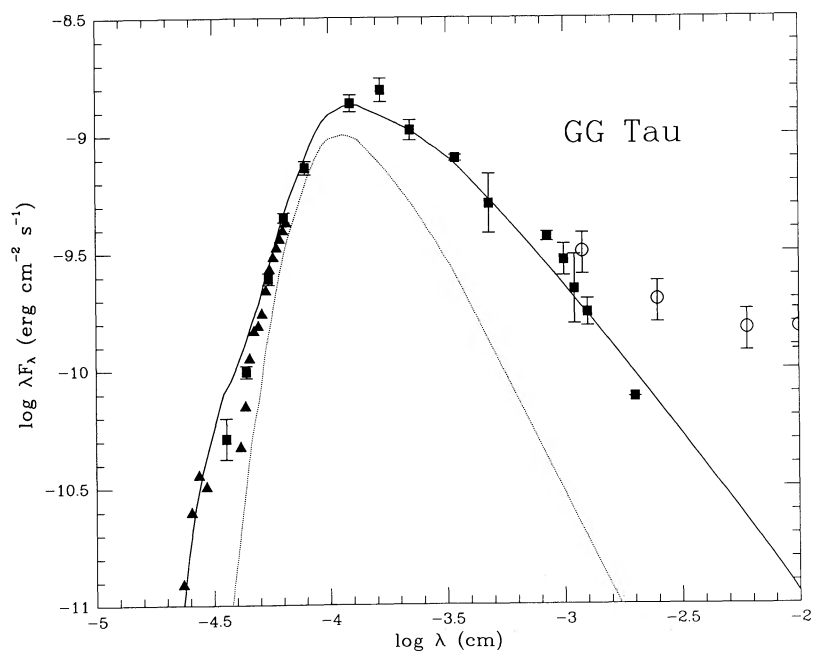


FIG. 7b

FIG. 7.—Models and observations of individual stars. The predicted and observed spectra for systems with the properties summarized in Tables 4 and 5. The solid line in each case is the predicted total flux and the dotted line is the stellar photospheric plus chromospheric flux. The filled triangles are the measured continuum values at a few wavelengths from contemporaneous *IUE* and Lick scanner spectrophotometry. The open triangles are similar observations with variability indicated by the error bars, either from ESO or from Rydgren *et al.* (1984) when ESO photometry was not available. The open circles are the *IRAS* PSC fluxes with the estimated 20% calibration accuracy indicated. No correction for extinction has been applied to data points; instead, the computed spectra are extinguished by the amount given in Table 4. The stars in this figure are those from region II of Fig. 5.

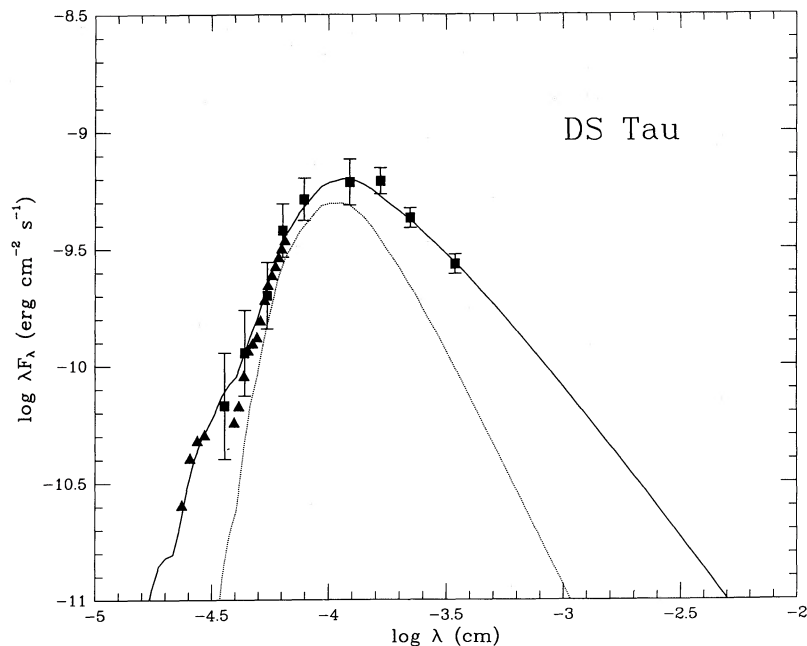


FIG. 7c

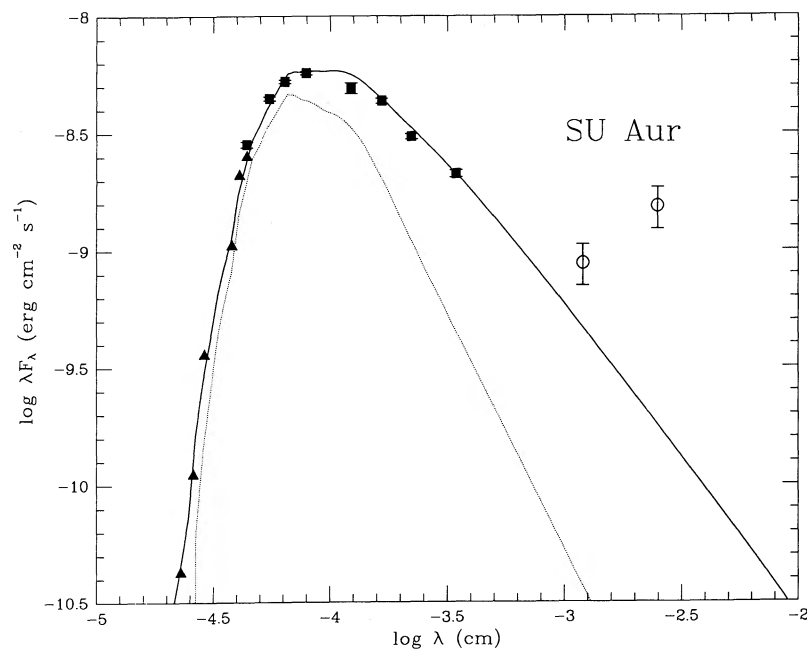


FIG. 7d

ultraviolet and optical spectra are shown together with computed models for the continuous energy distributions (see Tables 4 and 5). Data for the Balmer jump spectral region are not contemporaneous with the *IUE* and optical data. In particular, BP Tauri displays strong variations of the Balmer jump region between 1983 (*solid line*) and 1986 (*dotted line*). It is evident from this picture that the boundary layer luminosity is comparable to the stellar luminosity in both objects—in contrast to Kenyon and Hartmann's (1987) claim that there is no evidence for boundary layer emission (and therefore for disk accretion) in typical T Tauri spectra.

Figure 7 displays the overall spectral energy distribution of each star. The various symbols used in this figure have the following meaning. The solid line in each case is the predicted total flux and the dotted line is the stellar photospheric flux. Note that extinction has been included in the computed energy distributions. The filled triangles are the measured continuum values at a few wavelengths from contemporaneous *IUE* and Lick scanner spectrophotometry. The open triangles are similar observations from Herbig and Goodrich (1986). The filled squares are photometric observations with variability indicated by the error bars, either from ESO or from Rydgren

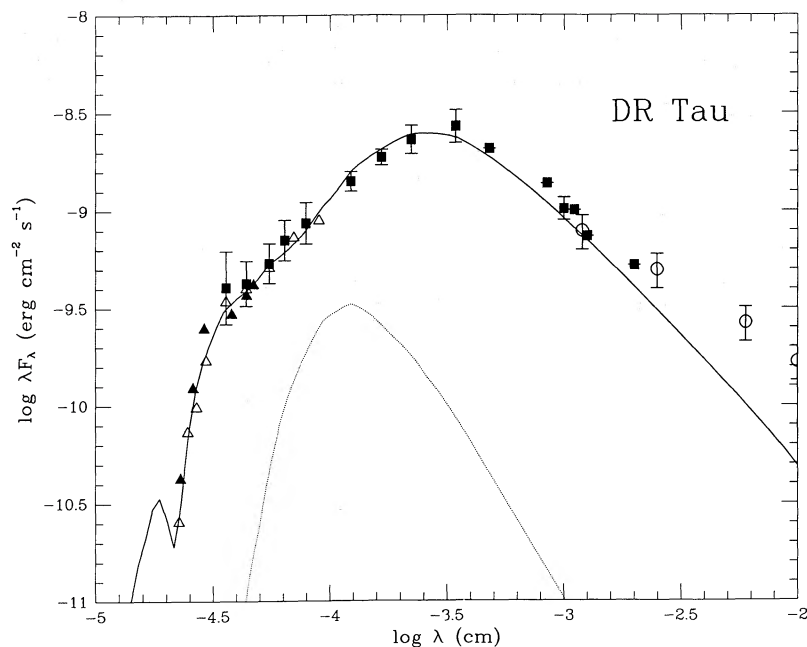


FIG. 8a

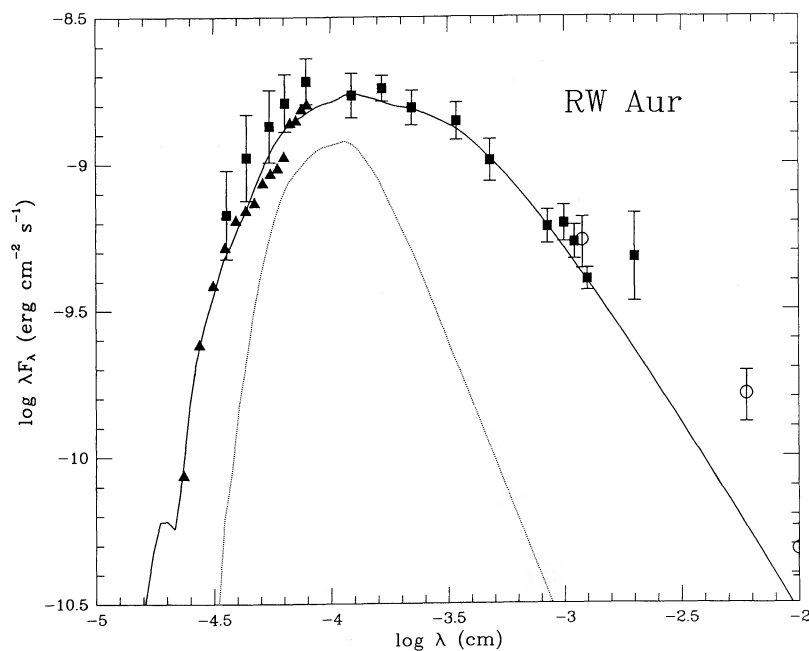


FIG. 8b

FIG. 8.—Same as Fig. 7 but for stars in region III of Fig. 6

et al. (1984) when ESO photometry was not available. The open circles are the *IRAS* PSC fluxes with the estimated 20% calibration accuracy indicated. Remarks on individual stars follow.

i) *BP Tauri*

BP Tauri is a K7 moderately active T Tauri star. Figures 6a and 7a illustrate the good agreement of the model with the observed energy distribution from 2500 Å to about 3.5 μm lends support to our suggestion that accretion is ultimately responsible for the continuum excesses in some classical T

Tauri stars. The *IRAS* data cannot be reproduced in the framework of our model, and we shall see below that the computed far-infrared flux of our models is often too low when compared to *IRAS* observations. This problem is discussed further in § VI.

ii) *GG Tauri*

We found it difficult to reproduce fluxes in the 3700–5000 Å range along with the strong ultraviolet (*IUE*) continuum of this K7 star within the framework of our boundary layer model. This is however not entirely surprising in view of Figure

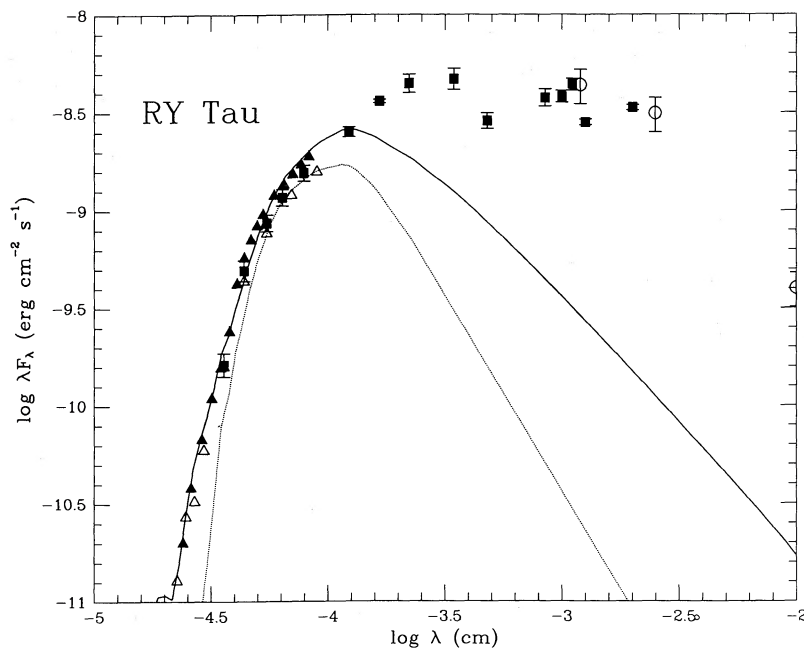


FIG. 8c

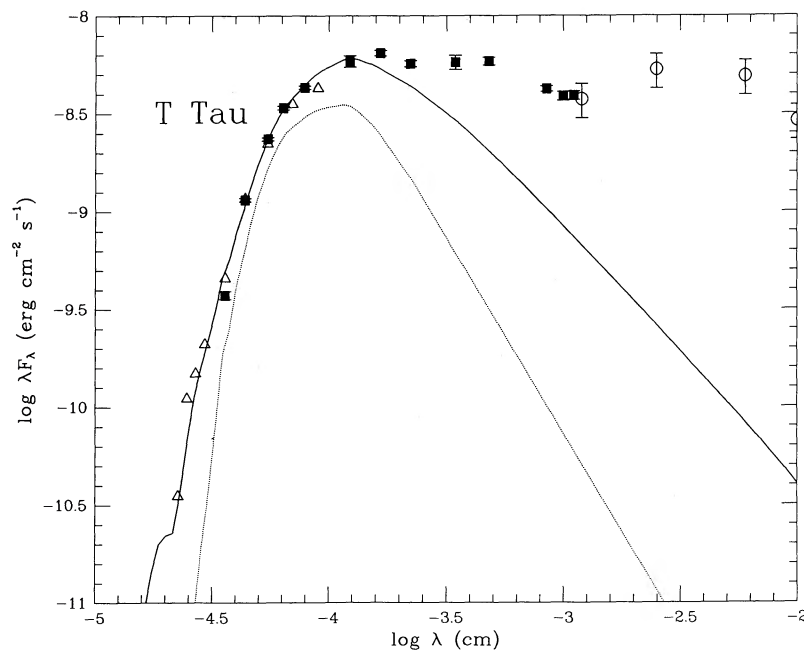


FIG. 8d

TABLE 5
MODELS FOR OBJECTS WITH KNOWN SPECTRAL TYPES

Star	(L_*/L_\odot)	(L_{acc}/L_*)	$(L_{\text{tot}}/L_{\text{obs}})$	T_{BL} (K)	f_{BL} (%)
BP Tau	2.04	0.80	2.30	8170	2.3
RY Tau	4.72	0.36	0.29	9540	1.6
T Tau	7.48	0.27	0.44	8580	1.8
DF Tau ^a	3.02	1.39	2.06	8730	2.8
GG Tau	2.77	1.01	2.42	8480	2.5
DS Tau	1.28	0.86	3.19	10500	1.6
SU Aur	9.62	0.12	1.08	7940	1.8

^a For $\dot{M} = 6.5 \times 10^{-7} M_\odot \text{ yr}^{-1}$.

6b, which reveals that the UV continuum is due at least in part to Balmer emission, not included in our simple model. A more detailed treatment of the boundary layer would be necessary; the *IUE* data obviously represent an upper limit to the optically thick emission from the boundary layer considered here. While this is true for all objects investigated here, it is only a problem for stars with strong Balmer jumps; in our sample these are GG Tau and, less critically, DF Tau and DS Tau.

The mismatch seen in Figure 7b between the infrared data in the 10–20 μm range, obtained with telescope aperture of a few arcseconds, and the *IRAS* measurements is somewhat puzzling. We suspect the presence of confusing sources in the 1'

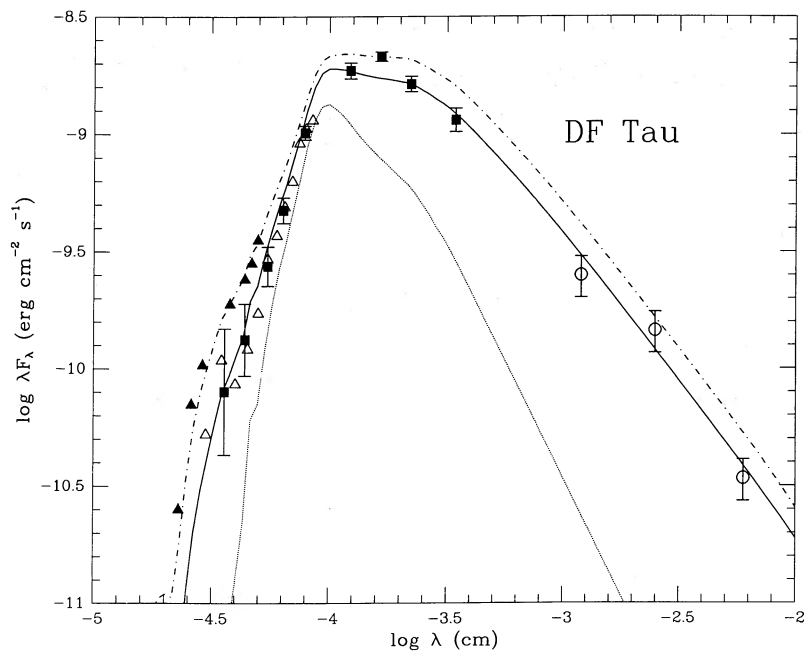


FIG. 9a

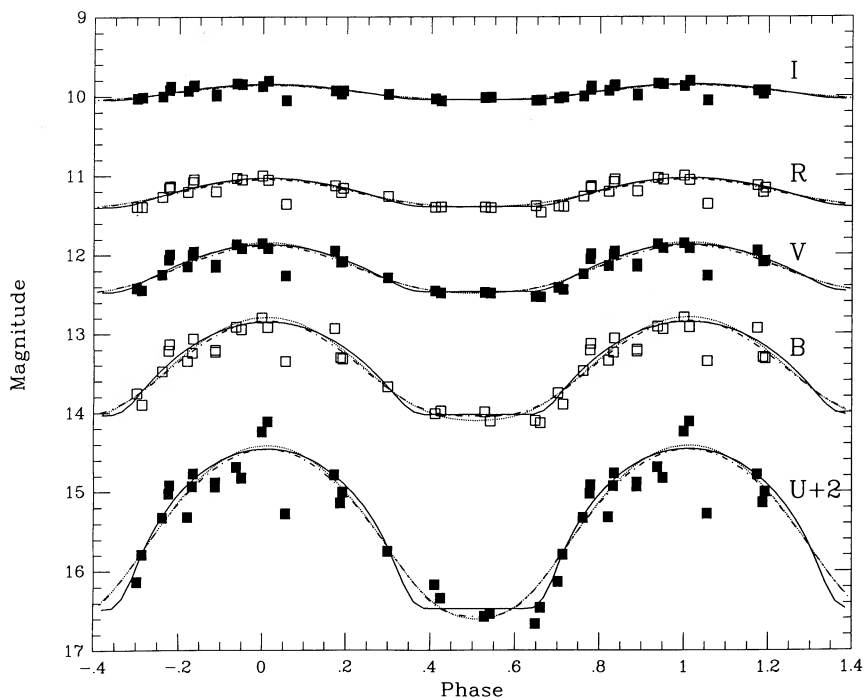


FIG. 9b

FIG. 9.—(a) Same as Fig. 7 for DF Tau, except that open triangles indicate selected continuum points of the 1986 spectrophotometry. (b) Light curves for DF Tau. The three smooth curves indicate three possible spot solutions with properties given in the text.

IRAS beam; Biegging, Cohen, and Schwartz (1984) reported the discovery of a radio source about $15''$ north of GG Tau, and they do not exclude the possibility that it is associated with an embedded young stellar object.

iii) *DS Tauri*

The faintest star in our sample, DS Tauri is not a point source in the *IRAS* catalog. As seen in Figure 7c, the accretion disk model gives a good fit to the overall spectral energy dis-

tribution of this K3 star except in the region of the Balmer jump, which is in emission (cf. the discussion of GG Tau). While faint, DS Tau is among the brightest YY Orionis stars as defined by Walker (1972) and the relevance of disk accretion to the YY Orionis phenomenon is discussed in § VI.

iv) *SU Aurigae*

This is one of the few T Tauri stars with G spectral type. Because its photosphere is much warmer than that of more

typical T Tauri stars, it contributes more to the ultraviolet part of the spectrum, with the result that the boundary layer emission is less prominent there. It is interesting here to test whether the chromosphere of a "naked" G2 T Tauri star (cf. Fig. 1) can possibly account for the observed ultraviolet excess of SU Aur. The dotted line of Figure 7*d* shows the contribution of both photosphere and chromosphere; and it obviously fails to account for the moderate ultraviolet excess of SU Aur. The accretion disk model, in contrast, is quite successful in reproducing the data, except for the *IRAS* points, which are again quite puzzling. SU Aur is a suspected spectroscopic binary system (Bouvier *et al.* 1986), but the secondary is probably too faint at all wavelengths to contribute significantly to the energy distribution.

b) Stars with $(K - L)_0 \geq 0.9$

Both extreme T Tauri stars with no visible photospheric spectrum (DR Tau and RW Aur) and moderately active stars with flat far-infrared excess (T Tau, RY Tau) are found in this subgroup, and DG Tau has the dubious privilege of being an extreme T Tauri star with flat far-infrared excess. We have so little information about the stellar component of DG Tau that we are unable to make meaningful models of this object, and we do not discuss it further here. Model parameters for the remaining objects are given in Table 4*b*, and observational data are displayed together with computed continuous energy distributions in Figure 8, where symbols have the same meaning as in Figure 7.

i) DR Tauri

Because of its wild spectroscopic and photometric variations, this star has attracted lots of attention in recent years (see Bertout [1984] and references therein). An average energy distribution constructed from several data sets is shown in Figure 8*a*. This energy distribution is unusual in that it peaks at L , and then decreases with a slope close to the value expected for an accretion disk. In fact, the overall spectrum is so close to that expected from an accretion disk that in our first models we had to artificially suppress the photospheric contribution in order to fit the observed data. Furthermore, the disk plus boundary layer system had to be seen face-on in order to maximize the ultraviolet and near-infrared contributions to the overall energy distribution.

Since DR Tauri has once been classified as a K5 star by Joy (1949), we then tried to add a late-type photosphere. It proved impossible to get a reasonable fit unless the photospheric radius was sizably smaller than the inner radius of the disk. The maximum stellar radius compatible with the data is about $1.2 R_{\odot}$, which, in the framework of our model, yields a V magnitude of about 13.5 to 14 for the stellar component, depending on the assumed extinction. Luckily, this is consistent with the magnitude that Joy (1949) recorded when he classified DR Tau as a K star, suggesting that the contribution from the disk to the optical spectrum was much smaller at that time. The brightness of DR Tau increased by 4–5 mag between 1960 and 1979 (see Chavarría 1979), and our model for the energy distribution suggests that the outburst results from a dramatic mass-accretion rate increase during the same period.

There are at least two possible reasons why DR Tauri's disk might not reach down to the stellar surface. Accretion might be magnetically dominated, as is suggested below for DF Tau, in which case the disk would be disrupted at a distance of a few stellar radii from the star; or the disk might be optically thin

close to the star. This could conceivably happen if α were large and if radiation from the boundary layer were providing additional heating to the disk's inner region, thus reducing the optical depth as seen in § II.

It seems difficult at this point to distinguish between these two possibilities. On one hand, the good fit to the UV data provided by the equatorial boundary layer may provide some support to the second hypothesis; but our models are less constrained for "extreme" T Tauri stars than for stars with visible photospheres. In addition to the two main parameters (i and \dot{M}), we can now adjust R_* and A_V almost at will, so that the derived properties of the boundary layer are subject to some uncertainty. On the other hand, the inner radius of the disk deduced from our models for this star is roughly consistent with the estimate of typical Alfvén radii for T Tauri stars (see eq. [18] below), so that the magnetic field could possibly disrupt the inner parts of the disk.

ii) RW Aurigae

A late G or early K spectral type has been occasionally observed in some spectrograms of this well-known extreme T Tauri star (e.g., Mundt and Giampapa 1982) and our best fit, displayed in Figure 8*b*, was indeed found for a K2 photosphere. Interestingly, we had to make the same assumptions as in the case of DR Tauri to find a good fit to the data. That is, we assumed that the stellar radius was significantly smaller than the inner disk radius and that the system was seen face-on. Thus, the above discussion of DR Tau applies to this star as well. Unfortunately, these were the only two extreme stars in our sample (disregarding here the flat-spectrum, extreme DG Tau), so that we cannot say at this point whether this emerging pattern applies to other extreme stars as well.

iii) T Tauri and RY Tauri

The flat far-infrared energy distributions of these two K1 stars cannot be reproduced in the framework of our model. Alternative models are discussed in § VI. Since both spectral types and extinction are known from the optical spectra of these objects, we can however deduce the maximum mass-accretion rate compatible with the ultraviolet and optical near-simultaneous data.

The inclination angle of T Tauri is well-determined from $v \sin i$ and the rotation period of 2.8 days (Herbst *et al.* 1987). Extinction values derived using the procedure outlined in § III are significantly smaller than the estimate of Cohen and Kuhi (1979) for these two stars. With the new extinction value, it proves possible to reproduce the energy distribution of T Tauri from the *IUE* range to the near-infrared with little optical veiling, in agreement with observations. RY Tauri's brightness underwent a large increase in 1983–1984, so that our ESO data could not be used together with the earlier spectrophotometric data. We thus averaged relevant data from Rydgren *et al.* (1984) to construct the optical and near-infrared energy distribution.

c) DF Tauri: Accretion Along Magnetic Field Lines?

DF Tauri is the only star for which all data, including the *IRAS* points, can be fitted by our simple model. The observed and computed energy distributions of DF Tau are displayed in Figure 9*a*. The 1983 spectrophotometric data (*filled triangles*) indicate a higher flux than do the 1984 photometric points (*filled squares*) and the 1986 spectrophotometry (*open triangles*). We thus present two models, which differ only in the adopted mass-accretion rate, to account for both sets of data.

Ironically, the observed light curve of that star (Fig. 9b) appears incompatible with the simple axisymmetric boundary layer model used in this investigation. In the following, we show that we might be witnessing magnetically controlled accretion.

The periodic light variations of DF Tau shown in Figure 9b suggest that accretion occurs on a single *hot spot* on the stellar surface. While many T Tauri stars occasionally display such periodicities they have been successfully reproduced by models of *dark spots* on the stellar surface (Bouvier and Bertout 1988). But the variations of the light-curve amplitude with wavelength observed in DF Tau can only be understood by assuming that the spot is brighter than the surrounding photosphere. We used our light-curve synthesis program to compute the properties of DF Tau's hot spot; three synthetic light curves are displayed together with the observations in Figure 9b. Acceptable solutions are found in the temperature range 6400–9100 K, in the angular radius range 6 to 13°, and for an inclination angle of the stellar rotation axis with respect to the observer in the range $40^\circ \leq i \leq 90^\circ$. Comparison of the spot properties with the boundary layer properties (cf. Table 5) suggests that the flux radiated away by the hot spot is roughly comparable to the radiative flux from the boundary layer.

Of course the simple boundary layer model of § II does not allow for nonaxisymmetric accretion. It is however well-known from the properties of accreting degenerate objects that if the magnetic field is large enough for the Alfvén radius to be larger than the stellar radius, the inner parts of the accretion disk will be disrupted and accretion will occur along magnetic field lines. If the magnetic field is dipolar, accretion will occur only onto the polar caps. Since the accretion energy is released in shocks close to the stellar photosphere, hot spots are formed on the polecaps and a periodic modulation of the light curve follows as soon as magnetic field symmetry axis and rotation axis are not aligned. If the field geometry is more complicated, as is likely here, accretion will occur along field lines intercepting the disk, and could result in a single spot if one large active region only is located in the vicinity of the equator.

The rough agreement between the flux radiated away by DF Tau's hot spot and the boundary layer flux necessary to explain the spectral energy distribution suggests that we are witnessing magnetically controlled accretion in DF Tauri. While the exact physics of accretion in that case are quite involved (cf. Arons, Klein, and Lea 1987), we can estimate DF Tau's Alfvén radius by equating the ram pressure of the accreting matter (assumed here to have reached free-fall velocity) to the magnetic pressure. Assuming that the magnetic moment μ in a large loop is given by $\mu = B_* R_*^3$, where B_* is the stellar magnetic field, we get

$$\mu^2 = (\mu_0/4\pi)R_M^{7/2}(2GM_*)^{1/2}\dot{M}, \quad (18)$$

There have been no successful detections of magnetic fields so far on T Tauri stars. Upper limits on the averaged longitudinal field are about 1000 Gauss, but it is probable that the complicated field geometries expected on T Tauri stars (Herbig and Soderblom 1980) would average out even if they were locally much stronger than the upper limit quoted above. In any case, a value of 2×10^3 Gauss does not appear unreasonable for active regions on late-type stars, in which case we find an Alfvén radius of about $5R_*$ from eq. 18.

Accretion along magnetic field lines may thus be a viable alternative to axisymmetric accretion in the case of DF Tau. We note that this star does not always display the periodic

light curve observed during the 1984 winter, although a preferred cycle length of 8.5 days seems often present (Bouvier and Bertout 1988); it is therefore probable that accretion proceeds in a nonsteady manner along temporally variable magnetic structures. Furthermore, accretion should be limited to active regions in the vicinity of the equator if a sizable stellar wind is to originate from DF Tauri's surface. Obviously, observational tests of this suggestion are possible. For example, if accretion is nonaxisymmetric and if the bulk of $H\alpha$ emission originates from the accretion region, as we argue below, we should expect some rotational modulation of $H\alpha$.

VI. DISCUSSION AND CONCLUSIONS

a) Average Properties of T Tauri Disks

We restrict the discussion to objects with visible photospheric spectra because disk parameters are best constrained for these. We include RY Tau and T Tau in this sample, although the accretion disk model is clearly unable to explain their entire spectral energy distributions. Since their ultraviolet and optical spectral regions are well fitted by our models, we shall assume here that a disk and boundary layer are present around these T Tauri stars. While the exact nature of disks surrounding T Tauri stars with flat infrared spectra might be different from the assumed one (see § Vb below), this should not affect the properties of the boundary layer, since the main assumption for its existence—namely that the matter within the disk is decelerated from some largely supersonic value to a much lower photospheric rotational velocity—is still fulfilled.

Our sample of seven stars with known spectral type is too small for a statistical analysis, yet average properties are helpful for envisioning a representative T Tauri disk. We first check that there is no obvious bias in the inclination angles used in the models. We find an average view angle of about 60° , a reasonable value since individual view angles are determined to about $\pm 10^\circ$ accuracy. Comparing the visual extinction values used for our best fits to the values derived from the optical data, we find an average extinction of 0.9 mag in both cases. We now turn to a brief analysis of the model properties summarized in Tables 4 and 5. The average mass-accretion rate for our seven stars is $2.1 \times 10^{-7} M_\odot \text{ yr}^{-1}$, and half of the accretion luminosity is dissipated in the boundary layer with area f_{BL} typically 2% of the stellar surface and temperature T_{BL} in the range 8000–10,000 K. The ratio of accretion to stellar luminosity L_{acc}/L_* (column [3] of Table 5) varies from 0.12 for the luminous G2 star SU Aur to 1.4 for DF Tau. Restricting ourselves to the four late-type stars which perhaps represent best the active T Tauri stars, we find that L_{acc}/L_* is about 1.0. It is therefore quite important to account for the energy sources extrinsic to the star in interpreting observations of such systems.

b) The Missing Far-Infrared Flux

We have seen in § V that the far-infrared fluxes predicted by the models are often lower than observed by *IRAS*. But column (4) of Table 5 demonstrates that the total system luminosity L_{tot} , i.e., the sum of stellar and accretion luminosities, is in most cases larger than the observed luminosity L_{obs} . This is because we have allowed for visual extinction in front of the system, but we have not considered the reemission of absorbed photons at longer wavelengths that would occur if extinction is due to dust in the vicinity of the star. In other words extinction is an energy sink in our model, as would be

the case if it were truly interstellar; an unlikely possibility since the Taurus cloud is so close to us. In fact, the moderate visual extinctions are likely to be intracloud rather than purely circumstellar, so that reprocessing will be by cool dust that emits mostly in the *IRAS* range and is included in the *IRAS* beam. We have not considered this process in detail because it would introduce several unknown parameters in our analysis. It is clear therefore that there is plenty of ultraviolet luminosity from the boundary layer which is not seen directly but which can easily appear as a far-infrared excess. The problem of missing infrared flux is acute only for RY Tau, T Tau, and DG Tau, i.e., stars with flat infrared spectra.

Kenyon and Hartmann (1987) and Adams, Lada, and Shu (1988) explore alternatives to the classical accretion disk in attempts to reproduce the far-infrared flat spectra of these stars while still retaining the basic hypothesis that a disk surrounds a single central star. Specifically, Kenyon and Hartmann suggest that the outer parts of the disk may be "flared-out," in which case a larger fraction of the stellar luminosity could be absorbed there and reemitted at long infrared wavelengths. Problems with this approach are discussed by Adams, Lada, and Shu, who show that the flat IR spectra can also be reproduced by assuming a flatter temperature distribution $T_D(r)$. While useful physical insight into the energy dissipation mechanism in the disk could be gained in this way, the complicated surroundings of most flat-spectra objects introduce further ambiguities.

For example, T Tauri is a triple system (Dyck, Simon, and Zuckerman 1982; Nisenson *et al.* 1985) that includes a mysterious infrared component (T Tauri South) which is probably responsible for much of the activity going on in the region (Weintraub, Masson, and Zuckerman 1987). The complexity of the region, which may also involve either a circumbinary disk or dense molecular condensations makes it likely that the observed overall spectrum in T Tauri's direction is actually a composite of several infrared sources. Another region of current strong interest, that of HL-XZ Tau, has proved in recent months to be quite complicated. Besides the two optical stars it involves a weak radio source and several new optical jets (R. Mundt, private communication). The picture of the close surroundings of optical young stars which emerges here is much more crowded than previously thought. Thus, it is probably worth keeping in mind that the flat infrared energy distribution observed toward some of the most exotic members of the T Tauri population might represent the composite spectrum of several sources.

c) Veiling

One of the clear predictions of the disk model is the extent of continuum veiling as a function of wavelength which will be masking the stellar photospheric spectrum due to the contributions of the disk (in the IR) and the boundary layer (in the UV). It has been known since Joy (1949) that there is dilution of absorption line strengths in some T Tauri stars; certain stars show so much dilution that no absorption lines are left visible. There have been several qualitative studies of the veiling since then. Rydgren, Strom, and Strom (1976) summarize several of the properties of the blue veiling, including (i) at least part of it looks like a true continuum, (ii) it roughly correlates with emission-line strength, (iii) it roughly correlates with the extent of variability, and (iv) it is consistent with Balmer and Paschen continuum emission. Other authors have suggested a differential veiling effect in which the strong lines fill in faster than the

weaker lines. This effect could arise from a stellar chromosphere. Recently both forms of veiling have been confirmed: continuum veiling by Walker (1987) who made a more quantitative analysis of scanner spectra, and differential veiling by Finkenzeller and Basri (1987) who showed that in stars of moderate activity the effect of the chromosphere on absorption lines can clearly be seen.

The situation is complicated somewhat by the demonstration of Calvet, Basri, and Kuhl (1984) that a sufficiently deep chromosphere can produce Balmer and Paschen continuum emission radiation. The question of whether there is both an active stellar atmosphere and an extrinsic source of continuum radiation depends on evaluating whether a chromosphere producing the observed line fluxes is strong enough to produce the continuum effects as well. It appears from the study of naked T Tauri chromospheres that this often is not the case. In none of these stars is the Balmer continuum observed to be in emission, yet the chromospheric lines are comparable in strength to the *chromospheric* components of some stars with disks (cf. § IIIa). Walker also notes that none of his four (moderate to extreme) T Tauri stars show the increase in emission-line strength that would be predicted by the chromospheric model to accompany the observed increase in continuum strength. These facts support our conclusion that there is evidence for an extrinsic source of blue continuum luminosity in a sizable fraction of the T Tauri population.

The current model is probably too simple to accurately predict the details of the veiling. For example, we noted earlier that it cannot predict a Balmer emission jump from the boundary layer, so that we will overestimate the mass-accretion rate (and hence the veiling) in cases where a strong Balmer jump is present. One should also realize that veiling and extinction are closely related in our models. For example, if the visual extinction of a given star is overestimated, then the mass accretion rate that will be required to reproduce the blue and UV continua will be larger than if A_V had its correct value, and the predicted veiling will be larger than it should be. The amount and wavelength dependence of veiling thus provide an excellent observational test of accretion models which can be made with optical spectra.

d) Remarks on YY Orionis Stars

YY Orionis stars, as defined by Walker (1972), are a subclass of T Tauri stars with strong ultraviolet excess (e.g., $U - B \leq 0$) which sometimes display inverse P Cygni profiles in their Balmer lines, although not in $H\alpha$. While the objects discussed by Walker are quite faint, a few brighter members of the subclass were discovered and studied in some detail, most notably S CrA (Appenzeller and Wolf 1977; Wolf, Appenzeller, and Bertout 1977; Edwards 1979; Bertout *et al.* 1982). In our sample, DS Tauri is the only typical YY Orionis star. A model based on *spherical* accretion of protostellar matter met with difficulties when it was realized that evidence for matter outflow was also present in many YY Ori stars. Mundt (1984) suggested that the inverse P Cygni features were caused by ejected matter which did not reach escape velocity and was falling back onto the star.

Mundt and Bastian's (1979) $(U - B)_0$ versus $(B - V)_0$ diagram reveals that most YY Ori stars are located, together with "normal" T Tauri stars, in the part of the diagram where we expect T Tauri stars to be surrounded by disks [i.e., in the region defined by $(U - B)_0 \leq 0$ and $(B - V)_0 \leq 1$; see § IV]. This suggests that YY Orionis stars are accreting from a disk,

and a reexamination of the available spectroscopic data in the light of this interpretation, while it is beyond the goals of this work, should prove fruitful. In particular, one needs to understand why YY Ori stars exhibit inverse P Cygni profiles while other accreting T Tauri stars do not; both the geometry of the accretion region and the disk's view angle probably play a role here. Additional spectroscopic observations of "normal" T Tauri stars located among the YY Ori stars in the $(U - B)_0$ versus $(B - V)_0$ diagram, particularly of those with predicted high mass-accretion rates, would also be helpful in this respect.

e) Balmer Lines: The Ultimate Test

While this work is concerned mainly with continuous radiative processes, a few words about the Balmer lines are in order since the disk model introduces new and severe constraints on the geometry of Balmer line formation region in T Tauri envelopes. As mentioned in the introduction, lack of red-displaced emission in the forbidden lines of many T Tauri stars led Appenzeller, Jankovics, and Oestreich (1984) and Edwards *et al.* (1987) to conclude that an optically thick disk was hiding the receding parts of the stellar wind. While the Balmer lines are formed much closer to the stars than the forbidden lines, the presence of an optically thick accretion disk extending down to the stellar surface should also result in lack of red-displaced Balmer emission, whereas the observed $H\alpha$ profiles of typical T Tauri stars have *extended red and blue wings* (see the superposed [O I] $\lambda 6300$ and $H\alpha$ lines profiles in Edwards *et al.* 1987).

Two possibilities then suggest themselves. (i) If the central disks regions are optically thin over a radial size comparable to or larger than the Balmer line formation region (which could happen for large viscosity and moderate accretion rates) then we can in principle retain the usual assumption that $H\alpha$ is formed in the wind (and perhaps partly in a chromosphere). (ii) If, however, the disk is optically thick down to the photosphere, the Balmer lines cannot be formed primarily in the wind.

Our models indicate that the optically thick disk reaches down to the stellar photosphere in most cases. In the few cases where magnetically controlled accretion is suggested, the inner disk radius compares well with the expected Alfvén radius of a few stellar radii. Formation of $H\alpha$ over a region extending farther out than the Alfvén radius will result in peculiar line profiles due to disk occultation effects. Computations to be published separately indeed indicate that profiles formed in a wind partially occulted by a disk have little in common with typical T Tauri $H\alpha$ profiles. We would therefore like to suggest here that contrary to an almost generally accepted view, Mg II and Balmer lines of T Tauri stars might not be primarily formed in the wind.

An additional piece of evidence for this controversial suggestion is the observed strong correlations between the flux in the Ca II, Mg II, and $H\alpha$ lines (Calvet *et al.* 1985; Bouvier 1987), which would be most easily understood if all these lines were at least partially originating from the same region, as would be the case if Balmer line as well as Ca II and Mg II line emission originates in a "boundary layer chromosphere," i.e., in an optically thin, hot region surrounding the boundary layer and heated by dissipation of magnetic waves originating in the turbulent boundary layer (see also Kenyon and Hartmann 1987).

Forming the bulk of line emission in a boundary layer's atmosphere has obvious advantages. First, the combination of

both organized (rotational) and turbulent velocity fields present in that region will result in the large line widths of 200–400 km s⁻¹ typically observed in $H\alpha$. Second, the $H\alpha$ flux is not related to the wind mass-loss rate any more, a desirable feature since mass-loss rates derived from this emission-line flux have been a source of embarrassment for many years. Another puzzling feature of $H\alpha$ profiles, namely that their widths indicate wind velocities that are usually smaller than the escape velocity from the stellar surface, is also eliminated in this model. We can thus envision a modest stellar wind and a mass-loss rate perhaps in the $10^{-9} M_{\odot} \text{ yr}^{-1}$ range, as suggested by the observed radiative losses in the X-ray range. The blue-displaced absorption component often seen in $H\alpha$ could then arise in the low-excitation parts of the stellar wind, which would be more readily seen in absorption than in emission.

e) Summary

We have explored the extent to which the continuum spectral energy distributions of T Tauri stars from 0.2 to 10 μm can be explained by a simple model consisting of an active PMS star (resembling the naked T Tauri stars) and an active accretion disk (as in Lynden-Bell and Pringle 1974). The disk contributes both an infrared excess due to accretion energy dissipation and reprocessing of stellar light, and an ultraviolet excess from the boundary layer between disk and star where half of the total accretion luminosity is generated. By using contemporaneous observations and studies of the range of variability in this spectral range, we show that the simple model is remarkably good at predicting the range of continuum excesses observed in T Tauri stars, with accretion rates implied up to a few times $10^{-7} M_{\odot} \text{ yr}^{-1}$. The few T Tauri stars with flat infrared continua cannot be explained by this model alone, but there are reasons to believe the *IRAS* beam might be contaminated by infrared sources located in the vicinity of these stars.

The details of the disk model are developed for the T Tauri case. We discuss the parameters of such a model and show that there are six, however all but two of them can in principle be fixed independently (through knowledge of the star). These two are the inclination of the disk and the accretion rate (and independent constraints on the inclination are available when both the rotation period and rotational velocity for the star are known). Since both the infrared and ultraviolet continua are strongly affected by accretion, when both are known they serve to constrain the accretion rate fairly well in the context of the simple model. Further constraints are provided by the extent and wavelength dependence of the optical veiling of the photospheric spectrum which is predicted by the model. Analysis of the differential (by line strength) and continuous veiling in observed spectra will provide an additional fairly rigorous test of the models. The presence of a strong stellar chromosphere, while important, is shown to be something that can be treated independently and which does not weaken the conclusion that a significant fraction of "classical" T Tauri stars are currently accreting matter from a surrounding disk. It is remarkable that so many (and until recently mysterious) properties of the spectra from very young stars can be fitted with such a simple model and so few parameters.

Naturally, this is not the whole story. The flat infrared distributions from some stars are not yet accounted for in this picture. Likewise the model should be elaborated to attempt an explanation of the strong Balmer continuum and line emission often observed. It is particularly tantalizing that $H\alpha$ lines

usually exhibit a fairly symmetric component with roughly the velocity width expected from boundary layer turbulence. More accurate estimates of the extinction and stellar parameters will pin down the properties of the disks more accurately. Detailed studies of resolved line profiles for both veiling in the absorption lines and velocity structure in the emission lines are essential in further testing the model. Finally the theory of the boundary layer needs much improvement, especially on the size the layer should have and the vertical temperature structure necessary to generate the emission features in the spectrum. Eventually the effects of magnetic fields must be faced, particularly since disk material is descending on stars known to be quite active magnetically. It is clear that disk accretion on T Tauri stars is an idea whose time has come.

We would like to acknowledge discussions with members of

the Center for Star Formation Studies (NASA), including F. Adams, M. Cohen, D. Lin, and F. Shu. Others with whom we had fruitful interactions include S. Cabrit, S. Edwards, L. Hartmann, G. Herbig, J. Heyvaerts, S. Kenyon, J. Pringle, K. and S. Strom, and M. Walker. C. B. gratefully acknowledges the hospitality of the Berkeley Astronomy Department. Many useful comments from the referee led to an improved presentation of our results. Some of the observational data was gathered by others; we would particularly like to acknowledge P. Bouchet and C. L. Imhoff. We have made use of catalog data supplied through the NSSDC. This work was largely supported through NSF grant AST-84-14811 to the University of California, and by grants from the IUE Guest Observer program. Observations at the Lick Observatory are supported in part by NSF block grant AST-86-14510 to the University of California.

REFERENCES

- Adams, F., Lada, C. J., and Shu, F., 1987, *Ap. J.*, **312**, 788.
 ———, 1988, *Ap. J.*, **326**, 865.
 Adams, F., and Shu, F. 1986, *Ap. J.*, **308**, 836.
 Appenzeller, I., and Wolf, B. 1977, *Astr. Ap.*, **54**, 713.
 Appenzeller, I., Jankovics, I., and Oestreicher, R. 1984, *Astr. Ap.*, **141**, 108.
 Arons, J., Klein, R. I., and Lea, S. M. 1987, *Ap. J.*, **312**, 666.
 Basri, G. 1987, in *Proc. Fifth Cambridge Workshop on Cool Stars*, ed. J. Linsky and R. Stencel (New York: Springer-Verlag), in press.
 Basri, G., Finkenzeller, U., and Imhoff, C. L. 1988, in preparation.
 Beall, J. H. 1986, *Ap. J.*, **316**, 227.
 Bertout, C. 1984, *Rept. Prog. Phys.*, **47**, 111.
 ———, 1987, in *IAU Symposium No. 122* (Dordrecht: Reidel), in press.
 Bertout, C., Carrasco, L., Mundt, R., and Wolf, B. 1982, *Astr. Ap. Suppl.*, **47**, 419.
 Bessel, M. S. 1979, *Pub. A.S.P.*, **91**, 589.
 Bieging, J. H. 1984, *Ap. J.*, **286**, 591.
 Bieging, J. H., Cohen, M., and Schwartz, P. R. 1984, *Ap. J.*, **282**, 699.
 Bodenheimer, P. 1983, *Lecture Appl. Math.*, **20**, 141.
 Boss, A. 1987, *Ap. J.*, **316**, 721.
 Bouvier, J. 1987, Thèse de Doctorat, Université Paris VII.
 Bouvier, J., and Bertout, C. 1988, *Astr. Ap.*, submitted.
 Bouvier, J., Bertout, C., Benz, W., and Mayor, M. 1985, in *Nearby Molecular Clouds*, ed. G. Serra (*Lectures Notes in Physics* **237**), p. 222.
 ———, 1986, *Astr. Ap.*, **165**, 110.
 Bouvier, J., Bertout, C., and Bouchet, P. 1988, *Astr. Ap.*, submitted.
 Calvet, N., Basri, G., and Kuhl, L. V. 1984, *Ap. J.*, **277**, 725.
 Calvet, N., Basri, G., Imhoff, C. L., and Giampapa, M. S. 1985, *Ap. J.*, **293**, 575.
 Chavarría, C. 1979, *Astr. Ap.*, **79**, L18.
 Cohen, M., and Kuhl, L. V. 1979, *Ap. J. Suppl.*, **41**, 743.
 Cram, L. E. 1979, *Ap. J.*, **234**, 949.
 DeCampli, W. M. 1981, *Ap. J.*, **244**, 128.
 Dumont, S., Heidmann, N., Kuhl, L. V., and Thomas, R. N. 1973, *Astr. Ap.*, **29**, 199.
 Dyck, H. M., Simon, T., and Zuckerman, B. 1982, *Ap. J. (Letters)*, **255**, L103.
 Edwards, S. 1979, *Pub. A.S.P.*, **91**, 329.
 Edwards, S., Cabrit, S., Strom, S. E., Heyer, I., Strom, K. M., and Anderson, E., 1987, *Ap. J.*, **321**, 473.
 Finkenzeller, U., and Basri, G. 1987, *Ap. J.*, **318**, 823.
 Friedjung, M. 1985, *Astr. Ap.*, **146**, 366.
 Graham, J. A. 1982, *Pub. A.S.P.*, **94**, 244.
 Hartmann, L., Edwards, S., and Avrett, A. 1982, *Ap. J.*, **261**, 279.
 Hartmann, L., Hewett, R., Stahler, S., and Mathieu, R. 1986, *Ap. J.*, **309**, 275.
 Herbig, G. H. 1970, *Mém. Soc. Roy. Sci. Liège*, **19**, 13.
 Herbig, G. H., and Goodrich, R. W. 1986, *Ap. J.*, **309**, 294.
 Herbig, G. H., and Soderblom, D. R. 1980, *Ap. J.*, **242**, 628.
 Herbst, W., Booth, J. F., Chugainov, P. F., Zajtseva, G. V., Barksdale, W., Covino, E., Terranegra, L., Vittone, A., and Vrba, F. 1987, *Ap. J. (Letters)*, **310**, L71.
 Holzer, T. E., Fla, T., and Leer, E. 1983, *Ap. J.*, **275**, 808.
 Jacoby, G. H., Hunter, D. A., and Christian, C. A. 1984, *Ap. J. Suppl.*, **56**, 257.
 Johnson, H. L. 1964, *Bol. Obs. Tonantzintla y Tacubaya*, **3**, 305.
 Johnson, H. L., Mitchell, R. I., Iriarte, B., and Wisniewski, W. Z. 1966, *Comm. Lunar Planet. Lab.*, **63**.
 Joy, A. H. 1949, *Ap. J.*, **110**, 424.
 Kenyon, S. J., and Hartmann, L. 1987, *Ap. J.*, **323**, 714.
 Kley, W., and Hensler, G. 1987, *Astr. Ap.*, **172**, 124.
 Koornneef, J. 1983, *Astr. Ap. Suppl.*, **51**, 489.
 Kuhl, L. V. 1964, *Ap. J.*, **140**, 1409.
 Lada, C. J., and Wilking, B. A. 1984, *Ap. J.*, **287**, 610.
 Lin, D. N. C., and Papaloizou, J. 1985, in *Protostars and Planets II*, ed. D. C. Black and M. S. Matthews (Tucson: University of Arizona Press), p. 981.
 Lynden-Bell, D., and Pringle, J. E. 1974, *M.N.R.A.S.*, **168**, 603(LBP).
 Mendoza, V. E. E. 1968, *Ap. J.*, **151**, 977.
 Morfill, G., Tscharnuter, W. M., and Völk, H. J., 1985, in *Protostars and Planets II*, ed. D. C. Black and M. S. Matthews (Tucson: University of Arizona Press), p. 493.
 Mundt, R. 1984, *Ap. J.*, **280**, 749.
 Mundt, R., and Bastian, U. 1979, *Astr. Ap.*, **75**, L14.
 Mundt, R., and Giampapa, M. S. 1982, *Ap. J.*, **256**, 156.
 Myers, P. C., and Benson, P. J. 1983, *Ap. J.*, **266**, 309.
 Nisenson, P., Stachnik, R. V., Karovska, M., and Noyes, R. 1985, *Ap. J. (Letters)*, **297**, L17.
 Pringle, J. E. 1977, *M.N.R.A.S.*, **178**, 95.
 Pringle, J. E., and Savonije, G. J. 1979, *M.N.R.A.S.*, **187**, 777.
 Robertson, J. A., and Frank, J. 1986, *M.N.R.A.S.*, **221**, 279.
 Rucinski, S. M. 1986, *A.J.*, **90**, 2321.
 Rydgren, A. E., Strom, S. E., and Strom, K. M. 1976, *Ap. J. Suppl.*, **30**, 307.
 Rydgren, A. E., Schmelz, J. T., Zak, D. S., and Vrba, F. J. 1984, *Pub. US Naval Obs.*, **25**, P1.
 Sargent, A. I., and Beckwith, S. 1987, *Ap. J.*, **323**, 294.
 Savage, B. D., and Mathis, J. S. 1979, *Ann. Rev. Astr. Ap.*, **17**, 73.
 Shakura, N. I., and Sunyaev, R. A. 1973, *Astr. Ap.*, **24**, 337.
 Terebey, S., Shu, F., and Cassen, P. 1984, *Ap. J.*, **286**, 529.
 Tscharnuter, W. M., 1985, in *Birth and Infancy of Stars*, ed. R. Lucas, A. Omont, and R. Stora (Amsterdam: Elsevier).
 Tylanda, R. 1977, *Acta Astr.*, **27**, 235.
 ———, 1981, *Acta Astr.*, **31**, 127.
 Vardya, M. S. 1961, *Ap. J.*, **133**, 107.
 Vogel, S., and Kuhl, L. V. 1981, *Ap. J.*, **245**, 960.
 Walker, M. F. 1972, *Ap. J.*, **175**, 89.
 ———, 1987, *Pub. A.S.P.*, **99**, 392.
 Walter, F. 1987, *Pub. A.S.P.*, **99**, 31.
 Weintraub, D., Masson, C. R., and Zuckerman, B. 1987, *Ap. J.*, **320**, 336.
 Winkler, K. H., and Newman, M. N., 1980a, *Ap. J.*, **236**, 201.
 ———, 1980b, *Ap. J.*, **238**, 311.
 Wolf, B., Appenzeller, I., and Bertout, C. 1977, *Astr. Ap.*, **58**, 163.
 Wu, C.-C., et al. 1983, *IUE NASA Newsletter*, **22**.

GIBOR BASRI and CLAUDE BERTOUT: Astronomy Department, University of California, Berkeley, CA 94720

JÉRÔME BOUVIER: Institut d'Astrophysique, 98bis, Boulevard Arago, F 75014 Paris, France